# Numerical simulations of Vlasov-Maxwell equations for laser plasmas based on Poisson structure

Yingzhe Li, Nicolas Crouseilles, Yajuan Sun

# Numerical simulations of one laser-plasma model based on Poisson structure

**Yingzhe Li**[a,b], **Yajuan Sun**[a,b,*], **Nicolas Crouseilles**[c]

[a] *LSEC, Academy of Mathematics and Systems Science, Chinese Academy of Sciences, Beijing 100190, CHINA*
[b] *University of Chinese Academy of Sciences, Beijing 100049, CHINA*
[c] *Univ. Rennes, Inria Bretagne Atlantique & ENS Rennes, MINGuS.*

**Abstract**

In this paper, a bracket structure is proposed for the laser-plasma interaction model introduced in [19], and it is proved by direct calculations that the bracket is Poisson which satisfies the Jacobi identity. Then splitting methods in time are proposed based on the Poisson structure. For the quasi-relativistic case, the Hamiltonian splitting leads to three subsystems which can be solved exactly. The conservative splitting is proposed for the fully relativistic case, and three one-dimensional conservative subsystems are obtained. Combined with the splittings in time, in phase space discretization we use the Fourier spectral and finite volume methods. It is proved that the discrete charge and discrete Poisson equation are conserved by our numerical schemes. Numerically, some numerical experiments are conducted to verify good conservations for the charge, energy and Poisson equation.

*Keywords:* Laser-plasma interaction, Vlasov–Maxwell system, Poisson bracket, Hamiltonian splitting, Conservative splitting.

## 1. Introduction

The system of Vlasov–Maxwell (VM) equations is an important model to describe the interactive dynamics of charged particles with electromagnetic field. In this paper, we focus on a reduced VM system which is introduced

*Corresponding author
*Email address:* sunyj@lsec.cc.ac.cn (**Yajuan Sun**)

in [19, 24] to describe the laser-plasma interaction. This laser-plasma (LP) model describes the action of a laser wave, called pump, penetrating into a plasma and heating it. During this process, the electrons will be accelerated by plasma waves generated from laser-plasma interaction, or more precisely, from stimulated Raman scattering (SRS). A good understanding of this model will help to realize many new applications arising in high-field science including the fast ignition concept, and plasma based electron accelerator schemes.

The numerical computation of the VM system is known to be difficult because of its high dimension in phase space and the multi-scale nature. Particle in Cell (PIC) method has been a widely used method, the idea of which is based on approximating the distribution function of particles by a finite number of super particles [1, 4, 7, 15]. The main advantage of the PIC methods is its low computational cost. However, its numerical noise only decreases in $\mathcal{O}(1/\sqrt{N})$ w.r.t particle number $N$. In comparison, grid-based methods offer a good alternative to overcome this lack of precision, for instance the semi-Lagrangian methods [18, 13, 35], energy-conserving discontinuous Galerkin methods [10, 11], and so on. As for the LP model and its variants, there have been some research works [3, 5, 6, 8, 14, 20, 22, 24, 2, 3, 21, 36], in which mathematical analyses of the LP model, some numerical methods and one convergence analysis have been studied.

The physical models such as the Vlasov–Maxwell equations which describe the complex physical phenomena, usually have conservative properties. Hence, numerical methods with good conservation properties, high accuracy, and good long time behaviors are required. Geometric numerical methods proposed in [17, 23, 32] are designed for the purpose of preserving the underlying geometric structures of dynamical systems. By preserving the geometric properties inherited by the concerned system, geometric integration methods usually provide superior long time behavior in comparison with traditional numerical methods, and are thus more suitable for large-scale, long-term simulations. In the context of VM system, several structure preserving methods have recently emerged, such as grid based methods [12, 26], PIC methods [25, 30, 38], in which Hamiltonian splitting methods [16, 31, 37] play an important role.

In this paper, for the LP system we present the bracket structure to reformulate it. The bracket is then proved by direct calculations to satisfy the Jacobi identity which means that it is Poisson. Our Poisson bracket is also related to one Poisson bracket in [28] by a coordinate transformation. There

are some other references about the Hamiltonian structures of reduced models for laser plasma interaction [33, 34, 9]. However, the models (expressed with moments) considered are different from the LP model (kinetic) in this work, although similar techniques are used in the derivation of Poisson brackets. Moreover, the Casimir functions of the LP system and corresponding conservative properties are analyzed based on the Poisson bracket.

In this work, we consider the LP model in three cases with different Lorentz factors: non-relativistic, quasi-relativistic and fully relativistic. In physics, these three cases are used to describe different physical problems. For the the particles with high energy, their behaviors can be well described by the fully relativistic LP model. When the effects of ultra-relativistic electrons (velocity close to light velocity) are ignored, and the pump intensity is moderate, the motion of charged particles can be simulated by the quasi-relativistic LP model. If the plasma temperature and the intensity of pump wave are small enough, the non-relativistic LP model without considering relativistic effects can be used to describe the laser-plasma interaction. For the non-relativistic and quasi-relativistic cases, implementing Hamiltonian splitting leads to three subsystems which can be solved *exactly*. Composing the exact solution of each subsystem provides the temporal discretizations enjoying the following properties: $(i)$ they are poisson, i.e., they can preserve the poisson structure of the LP model; $(ii)$ they can be generalized to have arbitrary high order by various composition methods; $(iii)$ they can be combined with any approximations in phase space. In the fully relativistic case, however, there is more difficulties: second order spatial derivatives and nonlinear source terms appears in the electromagnetic field equations, and the Lorentz factor depends on the momentum and space at the same time. This relativistic factor makes some subsystems derived by Hamiltonian splitting can not be solved exactly and two dimensional reconstruction is need in numerical computation. By rewriting the Vlasov equation in the conservative formulation, we propose a new splitting which gives three one dimensional conservative subsystems. One important property of the two splittings proposed in this paper is that the discrete charge and Poisson equation are conserved.

The paper is organized as follows. In section 2 we introduce the LP system and its Poisson structure. In section 3, phase space discretizations of the LP system are described. In section 4, two splitting methods are proposed for the LP system in order to derive the temporal discretizations. In section 5, several numerical experiments are given to validate the long term behaviors

of our schemes. Finally, we conclude this paper.

## 2. The Hamiltonian structure of laser-plasma model

The starting point of the derivation of the LP model is a VM system with one dimension in space (called $x$) and three dimensions in momentum. To describe the laser-plasma interaction, we can assume the motions of charged particles are faster along the propagation direction of laser than in the associated transversal direction. An important property is $\mathbf{p}_\perp + \mathbf{A}_\perp(x,t) = \text{const}$ ($\perp$ means the transversal direction of the laser). Therefore, the four-dimensional VM system can be reduced to a two-dimensional LP model considered in this paper. Refer to [3, 19, 24] for more details.

The main goal of this section is to introduce the LP model and its Hamiltonian structure. The LP model is described by the following reduced VM equations

$$\frac{\partial f}{\partial t} + \frac{p}{\gamma_1}\frac{\partial f}{\partial x} + \left(E_x - \frac{\mathbf{A}_\perp}{\gamma_2}\cdot\frac{\partial \mathbf{A}_\perp}{\partial x}\right)\frac{\partial f}{\partial p} = 0, \tag{1}$$

$$\frac{\partial \mathbf{A}_\perp}{\partial t} = -\mathbf{E}_\perp, \tag{2}$$

$$\frac{\partial E_x}{\partial t} = -\int_{\mathbb{R}} \frac{p}{\gamma_1} f(x,p,t)\,\mathrm{d}p + \bar{J}(t), \tag{3}$$

$$\frac{\partial \mathbf{E}_\perp}{\partial t} = -\frac{\partial^2 \mathbf{A}_\perp}{\partial x^2} + \mathbf{A}_\perp \int_{\mathbb{R}} \frac{1}{\gamma_2} f(x,p,t)\mathrm{d}p, \tag{4}$$

$$\frac{\partial E_x}{\partial x} = \int_{\mathbb{R}} f(x,p,t)\mathrm{d}p - 1, \tag{5}$$

where $f(x,p,t)$ is the particle distribution function with $x \in \Omega \subset \mathbb{R}$ the spatial variable, $p \in \mathbb{R}$ the momentum variable, and $t \geq 0$ time. Denote the electric field and vector potential by $\mathbf{E} = (E_x, \mathbf{E}_\perp)$ and $\mathbf{A} = (0, \mathbf{A}_\perp)$, where $E_x = E_x(x,t)$ is the longitudinal component of electric field at the $x$ direction, $\mathbf{E}_\perp = (E_y, E_z)$ and $\mathbf{A}_\perp = (A_y, A_z)$ are the transverse components of electric field and vector potential (pump wave). $\gamma_1$ and $\gamma_2$ denote two relativistic parameters: $\gamma_1 = \gamma_2 = 1$ in the nonrelativistic case; $\gamma_1 = \sqrt{1+p^2}$, $\gamma_2 = 1$ in the quasi-relativistic case; and $\gamma_1 = \gamma_2 = \sqrt{1+p^2+|\mathbf{A}_\perp|^2}$ in the fully relativistic case. Here $\cdot$ represents the scalar product in $\mathbb{R}^2$, and $\bar{J}(t) = \frac{1}{|\Omega|}\int_{\Omega\times\mathbb{R}} \frac{p}{\gamma_1} f(x,p,t)\mathrm{d}x\mathrm{d}p$ guarantees the zero average property of $E_x$,

i.e.,

$$\int_\Omega E_x(x,t)\mathrm{d}x = 0, \ \ \forall t \geq 0. \tag{6}$$

Denote by $\mathcal{M}$ the infinite-dimensional manifold with coordinate ($f$, $E_x$, $\mathbf{E}_\perp$, $\mathbf{A}_\perp$). For arbitrary two functionals $\mathcal{F}$, $\mathcal{G}$ defined on $\mathcal{M}$, we present the following Poisson bracket for the LP system

$$\begin{aligned}\{\mathcal{F},\mathcal{G}\} = &\int_{\Omega\times\mathbb{R}} f\left[\frac{\delta\mathcal{F}}{\delta f},\frac{\delta\mathcal{G}}{\delta f}\right]_{xp}\mathrm{d}x\mathrm{d}p \ + \int_{\Omega\times\mathbb{R}}\left(\frac{\delta\mathcal{F}}{\delta E_x}\frac{\partial f}{\partial p}\frac{\delta\mathcal{G}}{\delta f} - \frac{\delta\mathcal{G}}{\delta E_x}\frac{\partial f}{\partial p}\frac{\delta\mathcal{F}}{\delta f}\right)\mathrm{d}x\mathrm{d}p \\ &+ \int_\Omega\left(\frac{\delta\mathcal{G}}{\delta\mathbf{A}_\perp}\cdot\frac{\delta\mathcal{F}}{\delta\mathbf{E}_\perp} - \frac{\delta\mathcal{F}}{\delta\mathbf{A}_\perp}\cdot\frac{\delta\mathcal{G}}{\delta\mathbf{E}_\perp}\right)\mathrm{d}x,\end{aligned} \tag{7}$$

where $[\cdot,\cdot]_{xp}$ is the Lie bracket defined by $[h,g]_{xp} = \partial_x h\partial_p g - \partial_p h\partial_x g$ for any two smooth functions $h(x,p)$ and $g(x,p)$. In the above bracket (7), $\frac{\delta\mathcal{F}}{\delta g}$ denotes the Fréchet derivative or functional derivative[1] of $\mathcal{F}$ about $g$, $g = f, E_x, \mathbf{E}_\perp, \text{or } \mathbf{A}_\perp$.

**Proposition 2.1** *The bracket defined in (7) is a Poisson bracket.*

Proof. It is easy to prove that the bracket is bilinear, skew symmetric, and satisfies Leibniz identity. As follows, we prove that the bracket defined in (7) satisfies the Jacobi identity for arbitrary functionals $\mathcal{F},\mathcal{G},\mathcal{H}$ defined on $\mathcal{M}$, i.e.,

$$\{\{\mathcal{F},\mathcal{G}\},\mathcal{H}\} + \{\{\mathcal{G},\mathcal{H}\},\mathcal{F}\} + \{\{\mathcal{H},\mathcal{F}\},\mathcal{G}\} = 0. \tag{8}$$

The bracket (7) can be denoted as

$$\{\mathcal{F},\mathcal{G}\} = \{\mathcal{F},\mathcal{G}\}_{xp} + \{\mathcal{F},\mathcal{G}\}_{AE} + \{\mathcal{F},\mathcal{G}\}_{fE_x} \tag{9}$$

with $\{\mathcal{F},\mathcal{G}\}_{xp} = \int_{\Omega\times\mathbb{R}} f[\frac{\delta\mathcal{F}}{\delta f},\frac{\delta\mathcal{G}}{\delta f}]_{xp}\mathrm{d}x\mathrm{d}p$, $\{\mathcal{F},\mathcal{G}\}_{AE} = \int_\Omega\left(\frac{\delta\mathcal{G}}{\delta\mathbf{A}_\perp}\cdot\frac{\delta\mathcal{F}}{\delta\mathbf{E}_\perp} - \frac{\delta\mathcal{F}}{\delta\mathbf{A}_\perp}\cdot\frac{\delta\mathcal{G}}{\delta\mathbf{E}_\perp}\right)\mathrm{d}x$ and $\{\mathcal{F},\mathcal{G}\}_{fE_x} = \int_{\Omega\times\mathbb{R}}\left(\frac{\delta F}{\delta E_x}\frac{\partial f}{\partial p}\frac{\delta G}{\delta f} - \frac{\delta G}{\delta E_x}\frac{\partial f}{\partial p}\frac{\delta F}{\delta f}\right)\mathrm{d}x\mathrm{d}p$. Then, the terms on the

[1]Note that the for the Fréchet derivative with respect to $E_x$, we need consider the zero average property of of $E_x$ (6).

left side of (8) can be written as

$$
\begin{aligned}
&\{\{\mathcal{F},\mathcal{G}\},\mathcal{H}\}+\text{cyc}\\
&=\{\{\mathcal{F},\mathcal{G}\}_{xp},\mathcal{H}\}+\{\{\mathcal{F},\mathcal{G}\}_{AE},\mathcal{H}\}+\{\{\mathcal{F},\mathcal{G}\}_{fE_x},\mathcal{H}\}+\text{cyc}\\
&=\underbrace{\{\{\mathcal{F},\mathcal{G}\}_{xp},\mathcal{H}\}_{xp}}_{1}+\underbrace{\{\{\mathcal{F},\mathcal{G}\}_{xp},\mathcal{H}\}_{AE}}_{2}+\underbrace{\{\{\mathcal{F},\mathcal{G}\}_{xp},\mathcal{H}\}_{fE_x}}_{3}\\
&+\underbrace{\{\{\mathcal{F},\mathcal{G}\}_{AE},\mathcal{H}\}_{xp}}_{4}+\underbrace{\{\{\mathcal{F},\mathcal{G}\}_{AE},\mathcal{H}\}_{AE}}_{5}+\underbrace{\{\{\mathcal{F},\mathcal{G}\}_{AE},\mathcal{H}\}_{fE_x}}_{6}\\
&+\underbrace{\{\{\mathcal{F},\mathcal{G}\}_{fE_x},\mathcal{H}\}_{xp}}_{7}+\underbrace{\{\{\mathcal{F},\mathcal{G}\}_{fE_x},\mathcal{H}\}_{AE}}_{8}+\underbrace{\{\{\mathcal{F},\mathcal{G}\}_{fE_x},\mathcal{H}\}_{fE_x}}_{9}+\text{cyc},
\end{aligned}
\tag{10}
$$

where 'cyc' denotes the cyclic permutation. By the bracket theorem presented in [29], we only need to consider the functional derivatives of $\{\mathcal{F},\mathcal{G}\}$ modulo the second derivative terms, which, with abuse of notations, gives

$$
\frac{\delta\{\mathcal{F},\mathcal{G}\}_{xp}}{\delta f}=\left[\frac{\delta\mathcal{F}}{\delta f},\frac{\delta\mathcal{G}}{\delta f}\right]_{xp},\ \frac{\delta\{\mathcal{F},\mathcal{G}\}_{xp}}{\delta\mathbf{E}_\perp}=\mathbf{0},\ \frac{\delta\{\mathcal{F},\mathcal{G}\}_{xp}}{\delta\mathbf{A}_\perp}=\mathbf{0},\ \frac{\delta\{\mathcal{F},\mathcal{G}\}_{xp}}{\delta E_x}=0,
\tag{11}
$$

$$
\frac{\delta\{\mathcal{F},\mathcal{G}\}_{AE}}{\delta f}=0,\ \frac{\delta\{\mathcal{F},\mathcal{G}\}_{AE}}{\delta\mathbf{E}_\perp}=\mathbf{0},\ \frac{\delta\{\mathcal{F},\mathcal{G}\}_{AE}}{\delta\mathbf{A}_\perp}=\mathbf{0},\ \frac{\delta\{\mathcal{F},\mathcal{G}\}_{AE}}{\delta E_x}=0,
\tag{12}
$$

$$
\frac{\delta\{\mathcal{F},\mathcal{G}\}_{fE_x}}{\delta f}=-\frac{\delta\mathcal{F}}{\delta E_x}\frac{\partial}{\partial p}\frac{\delta\mathcal{G}}{\delta f}+\frac{\delta\mathcal{G}}{\delta E_x}\frac{\partial}{\partial p}\frac{\delta\mathcal{F}}{\delta f},
\tag{13}
$$

$$
\frac{\delta\{\mathcal{F},\mathcal{G}\}_{fE_x}}{\delta\mathbf{E}_\perp}=\mathbf{0},\ \frac{\delta\{\mathcal{F},\mathcal{G}\}_{fE_x}}{\delta\mathbf{A}_\perp}=\mathbf{0},\ \frac{\delta\{\mathcal{F},\mathcal{G}\}_{fE_x}}{\delta E_x}=0.
\tag{14}
$$

With the above equalities, the following assertions are the immediate consequences:

- Term $1+\text{cyc}$ vanishes because $\{\mathcal{F},\mathcal{G}\}_{xp}$ is the Lie Poisson bracket of the Vlasov–Poisson system (see [27]).
- Term 2 vanishes due to the second and third equations in Eq. (11).
- Terms $4,5,6$ vanish when Eq. (12) is used.
- Term 8 vanishes because of the first and second equations in Eq. (14).

The remaining terms in (10) labelled as 3, 7, and 9 are proven to be cancelled out in Appendix A. This completes the proof of this proposition. □

With this Poisson bracket, the LP system (1-4) can be reformulated as a Poisson system

$$\dot{\mathcal{Z}} = \{\mathcal{Z}, \mathcal{H}\} \tag{15}$$

with the corresponding Hamiltonian

$$\mathcal{H} = K + \frac{1}{2}\int_\Omega |\mathbf{E}|^2 \mathrm{d}x + \frac{1}{2}\int_\Omega \left|\frac{\partial \mathbf{A}}{\partial x}\right|^2 \mathrm{d}x. \tag{16}$$

In (16), $K$ denotes the kinetic energy which is $K = \frac{1}{2}\int_{\Omega\times\mathbb{R}} (p^2 + |\mathbf{A}_\perp|^2) f \mathrm{d}x\mathrm{d}p$ in non-relativistic case, $K = \int_{\Omega\times\mathbb{R}} (\gamma_1 - 1 + \frac{|\mathbf{A}_\perp|^2}{2}) f \mathrm{d}x\mathrm{d}p$ in quasi-relativistic case, and $K = \int_{\Omega\times\mathbb{R}} (\gamma_1 - 1) f \mathrm{d}x\mathrm{d}p$ in fully relativistic case.

Let $\mathcal{M}_1$ be an infinite-dimensional manifold with coordinate $(f_M, \mathbf{A}, \mathbf{Y})$. Here, $f_\mathrm{M}$ is a function of $(x, P, t)$ defined by $f_\mathrm{M}(x, P, t) := f(x, P - A_x, t)$, $\mathbf{Y}$ is a function of $x$ by $\mathbf{Y}(x) := -\mathbf{E}(x)$. Then we have the following proposition.

**Proposition 2.2** *The Poisson bracket on $\mathcal{M}$ defined in (7) can be connected to the Poisson bracket on $\mathcal{M}_1$ by*

$$\begin{aligned}\{\{\bar{\mathcal{F}}, \bar{\mathcal{G}}\}\}(f_\mathrm{M}, \mathbf{A}, \mathbf{Y}) := &\int_{\Omega\times\mathbb{R}} f_\mathrm{M}(x, P, t) \left[\frac{\delta \bar{\mathcal{F}}}{\delta f_\mathrm{M}}, \frac{\delta \bar{\mathcal{G}}}{\delta f_\mathrm{M}}\right]_{xP} \mathrm{d}x\mathrm{d}P \\ &+ \int_\Omega \left(\frac{\delta \bar{\mathcal{F}}}{\delta \mathbf{A}} \cdot \frac{\delta \bar{\mathcal{G}}}{\delta \mathbf{Y}} - \frac{\delta \bar{\mathcal{G}}}{\delta \mathbf{A}} \cdot \frac{\delta \bar{\mathcal{F}}}{\delta \mathbf{Y}}\right) \mathrm{d}x\end{aligned} \tag{17}$$

*for functionals $\bar{\mathcal{F}}$ and $\bar{\mathcal{G}}$ of $f_\mathrm{M}, \mathbf{A}, \mathbf{Y}$.*

Proof. Given a functional $\mathcal{F}(f, E_x, \mathbf{A}_\perp, \mathbf{E}_\perp)$, define $\bar{\mathcal{F}}(f_\mathrm{M}, \mathbf{A}, \mathbf{Y})$ by

$$\bar{\mathcal{F}}(f_\mathrm{M}, \mathbf{A}, \mathbf{Y}) := \mathcal{F}(f, -Y_x, \mathbf{A}_\perp, -\mathbf{Y}_\perp).$$

By the chain rules of functional derivative, we obtain

$$\frac{\delta \bar{\mathcal{F}}}{\delta f_\mathrm{M}} = \frac{\delta \mathcal{F}}{\delta f}, \quad \frac{\delta \bar{\mathcal{F}}}{\delta A_x} = \frac{\delta \mathcal{F}}{\delta f}\frac{\partial f}{\partial p}, \quad \frac{\delta \bar{\mathcal{F}}}{\delta \mathbf{A}_\perp} = \frac{\delta \mathcal{F}}{\delta \mathbf{A}_\perp}, \quad \frac{\delta \bar{\mathcal{F}}}{\delta \mathbf{Y}} = -\frac{\delta \mathcal{F}}{\delta \mathbf{E}}. \tag{18}$$

Substituting the above equalities into the right side of (17), gives

$$\begin{aligned}\{\{\bar{\mathcal{F}}, \bar{\mathcal{G}}\}\}(f_\mathrm{M}, \mathbf{A}, \mathbf{Y}) = &\int_{\Omega\times\mathbb{R}} f(x, p - A_x, t) \left[\frac{\delta \mathcal{F}}{\delta f}, \frac{\delta \mathcal{G}}{\delta f}\right]_{xp} \mathrm{d}x\mathrm{d}p \\ + \int_{\Omega\times\mathbb{R}} &\left(\frac{\delta \mathcal{F}}{\delta E_x}\frac{\partial f}{\partial p}\frac{\delta \mathcal{G}}{\delta f} - \frac{\delta \mathcal{G}}{\delta E_x}\frac{\partial f}{\partial p}\frac{\delta \mathcal{F}}{\delta f}\right) \mathrm{d}x\mathrm{d}p + \int_\Omega \left(\frac{\delta \mathcal{G}}{\delta \mathbf{A}_\perp} \cdot \frac{\delta \mathcal{F}}{\delta \mathbf{E}_\perp} - \frac{\delta \mathcal{F}}{\delta \mathbf{A}_\perp} \cdot \frac{\delta \mathcal{G}}{\delta \mathbf{E}_\perp}\right) \mathrm{d}x.\end{aligned} \tag{19}$$

Comparing (19) with (7) implies

$$\{\mathcal{F},\mathcal{G}\}(f,E_x,\mathbf{A}_\perp,\mathbf{E}_\perp)=\{\{\bar{\mathcal{F}},\bar{\mathcal{G}}\}\}(f_{\rm M},\mathbf{A},\mathbf{Y}).$$

This completes the proof of this proposition. □

The above proposition can be generalized to four-dimensional LP model [2, 21] by one similar coordinate transformation.

**Definition 2.1** *[27] A smooth functional $\mathcal{C}$ defined on $\mathcal{M}$ is called a Casimir functional for a given Poisson bracket $\{\cdot,\cdot\}$ if*

$$\{\mathcal{C},\mathcal{G}\}=0$$

*holds for arbitrary smooth functional $\mathcal{G}$.*

**Proposition 2.3** *The functional*

$$\mathcal{C}_{x_0}(\mathcal{Z})=\int_\Omega\frac{\partial E_x}{\partial x}\delta(x-x_0)\mathrm{d}x-\int_{\Omega\times\mathbb{R}}f\delta(x-x_0)\mathrm{d}x\mathrm{d}p,\quad x_0\in\Omega \tag{20}$$

*is a Casimir functional of the Poisson bracket (7).*

Proof. From (20), it is known that

$$\frac{\delta\mathcal{C}_{x_0}}{\delta f}(\mathcal{Z})=-\delta(x-x_0),\quad \frac{\delta\mathcal{C}_{x_0}}{\delta E_x}(\mathcal{Z})=-\frac{\partial\delta(x-x_0)}{\partial x},\quad \frac{\delta\mathcal{C}_{x_0}}{\delta\mathbf{E}_\perp}(\mathcal{Z})=\frac{\delta\mathcal{C}_{x_0}}{\delta\mathbf{A}_\perp}(\mathcal{Z})=\mathbf{0},$$

where $\delta$ is the generalized function. Inserting the above equality into (7) gives

$$\begin{aligned}\{\mathcal{C}_{x_0}(\mathcal{Z}),\mathcal{G}(\mathcal{Z})\}=&\int_{\Omega\times\mathbb{R}}\frac{\partial\delta(x-x_0)}{\partial x}\left(-f\frac{\partial}{\partial p}\frac{\delta\mathcal{G}}{\delta f}-\frac{\partial f}{\partial p}\frac{\delta\mathcal{G}}{\delta f}\right)\mathrm{d}x\mathrm{d}p\\&+\int_{\Omega\times\mathbb{R}}\frac{\delta\mathcal{G}}{\delta E_x}\frac{\partial f}{\partial p}\delta(x-x_0)\mathrm{d}x\mathrm{d}p.\end{aligned} \tag{21}$$

By using the integration by parts, it is clear that the first integral on the right side of Eq. (21) vanishes. As $f$ is compactly supported along $p$ direction and $\frac{\delta\mathcal{G}}{\delta E_x}$ is independent of $p$, the second integral on the right side of Eq. (21) is also 0. This implies that $\mathcal{C}_{x_0}$ is Casimir according to definition 2.1. □

**Proposition 2.4** *[27] Denote $\mathcal{F}(\mathcal{M})$ the set of smooth functionals on $\mathcal{M}$. For a given function $\Phi : \mathbb{R} \to \mathbb{R}$, the functional $\mathcal{C} : \mathcal{F}(\mathcal{M}) \to \mathbb{R}$ defined as*

$$\mathcal{C}(f) = \int_{\Omega \times \mathbb{R}} \Phi(f(x,p)) \mathrm{d}x\mathrm{d}p, \tag{22}$$

*is a Casimir functional of the Poisson bracket (7).*

Based on the Poisson structure (7), in the following sections splitting methods are constructed for the LP system.

## 3. Phase space discretization

In this section, we present the phase space discretizations for the LP system. With the assumption that the LP system is periodic in $x$ direction with period $L$, we can take the computational domain in phase space as $\Omega \times \Omega_p = [0, L] \times [-P_L, P_R]$ with $P_L, P_R$ large enough to guarantee that $f$ is sufficiently small at $\Omega \times \partial\Omega_p$. In the following sections, periodic boundary conditions are imposed at the boundary of $\Omega \times \Omega_p$. Choosing the uniform grids gives

$$\begin{aligned} x_j &= (j-1)\Delta x, \quad j = 1, \ldots, M, \quad \Delta x = L/M, \\ p_{\ell-1/2} &= (\ell-1)\Delta p - P_L \quad \ell = 1, \ldots, N, \quad \Delta p = (P_R + P_L)/N. \end{aligned}$$

Firstly, we present the spatial discretizations for $E_x, \mathbf{E}_\perp, \mathbf{A}_\perp$. Let us give the detail for approximating $E_x$, the same strategy can be used for discretizing $\mathbf{E}_\perp$ and $\mathbf{A}_\perp$. Denote the discrete value of $E_x$ at $(x_j, t)$ by $E_{x,j}(t)$. We use the spectral Fourier expansion to approximate $E_x$ due to the periodicity of $E_x$. It reads

$$E_{x,j}(t) = \sum_{k=-M/2+1}^{M/2} \hat{E}_{x,k}(t) e^{2\pi \mathrm{i} jk/M}, \tag{23}$$

where $j = 1, \ldots, M$ and $\mathrm{i} = \sqrt{-1}$. To discretize the distribution function $f$ in phase space, we use a spectral representation in $x$ direction while a finite-volume discretization is used for the momentum $p$ direction. Use $f_\ell(x,t)$ to denote the average of $f(x,p,t)$ over a cell $P_\ell = [p_{\ell-1/2}, p_{\ell+1/2}]$, it is

$$f_\ell(x,t) := \frac{1}{\Delta p} \int_{P_\ell} f(x,p,t)\, \mathrm{d}p.$$

Combining it with the Fourier expansion in $x$-variable gives the approximation solution of $f$ at $(x_j, p_\ell)$ with $p_\ell = (\ell - \frac{1}{2})\Delta p - P_L$ that

$$f_{j,\ell}(t) = \sum_{k=-M/2+1}^{M/2} \hat{f}_{k,\ell}(t) e^{2\pi \mathrm{i} jk/M}. \tag{24}$$

To evaluate the off-grid value of $f$ in $p$ direction, here we use the so-called parabolic spline method (PSM) introduced in [39] to reconstruct a continuous function by using $f_{j,\ell}$ and periodic boundary condition. It has been pointed out in [13, 39] that using PSM for reconstructing $f$ is equivalent to applying the cubic spline interpolation for the primitive function of $f$. Specifically, for a simple advection problem (independent variable $x$ is omitted),

$$\frac{\partial f}{\partial t} + a\frac{\partial f}{\partial p} = 0, \quad a > 0$$

we have

$$f_\ell(t) = \frac{1}{\Delta p}\int_{p_{\ell-\frac{1}{2}}}^{p_{\ell+\frac{1}{2}}} f(p,t)\mathrm{d}p = \frac{1}{\Delta p}\int_{p_{\ell-\frac{1}{2}}-at}^{p_{\ell+\frac{1}{2}}-at} f_0(p)\mathrm{d}p, \tag{25}$$

where $f_0(p)$ is the initial condition which is a piecewise polynomial reconstructed from the values $f_\ell(0)$, $\ell = 1, \ldots, N$ by using PSM. The last equality of (25) holds as the solution $f$ of this advection system is $f(p,t) = f_0(p-at)$. The reconstruction of $f$ can be obtained by other approaches. The advantage of using parabolic spline method is that it can preserve the charge, that is

$$\int_{-P_L}^{P_R} f(p,0)\mathrm{d}p = \sum_{\ell=1}^{N} f_\ell(0)\Delta p. \tag{26}$$

## 4. Numerical discretizations

In this section, splitting methods are constructed for the LP system based on the Poisson bracket derived above. As there is no intrinsic difference between non-relativistic case and quasi-relativistic case, we here concentrate on quasi-relativistic, and fully relativistic cases. Combined with the phase space discretizations presented in the previous section, fully numerical discretizations are obtained.

*4.1. Quasi-relativistic case*

In the quasi-relativistic case $\gamma_1 = \sqrt{1+p^2}$ and $\gamma_2 = 1$, from (16) we know that the Hamiltonian has a form of

$$\begin{aligned}\mathcal{H}(f, E_x, \mathbf{E}_\perp, \mathbf{A}_\perp) =& \frac{1}{2}\int_\Omega (E_x^2 + |\mathbf{E}_\perp|^2)\mathrm{d}x + \int_{\Omega\times\mathbb{R}} (\sqrt{1+p^2}-1) f \mathrm{d}x\mathrm{d}p \\ &+ \frac{1}{2}\int_\Omega \left|\frac{\partial \mathbf{A}_\perp}{\partial x}\right|^2 \mathrm{d}x + \frac{1}{2}\int_{\Omega\times\mathbb{R}} |\mathbf{A}_\perp|^2 f \mathrm{d}x\mathrm{d}p.\end{aligned} \tag{27}$$

By investigation, the Hamiltonian (27) can be decomposed as

$$\mathcal{H} = \mathcal{H}_E + \mathcal{H}_A + \mathcal{H}_p,$$

where $\mathcal{H}_E = \frac{1}{2}\int_\Omega (E_x^2 + |\mathbf{E}_\perp|^2)\mathrm{d}x$, $\mathcal{H}_A = \frac{1}{2}\int_{\Omega\times\mathbb{R}} |\mathbf{A}_\perp|^2 f \mathrm{d}x\mathrm{d}p + \frac{1}{2}\int_\Omega \left|\frac{\partial \mathbf{A}_\perp}{\partial x}\right|^2 \mathrm{d}x$, and $\mathcal{H}_p = \int_{\Omega\times\mathbb{R}} \left(\sqrt{1+p^2}-1\right) f \mathrm{d}x\mathrm{d}p$, and three subsystem can be obtained,

$$\dot{\mathcal{Z}} = \{\mathcal{Z}, \mathcal{H}_E\}, \quad \dot{\mathcal{Z}} = \{\mathcal{Z}, \mathcal{H}_A\}, \quad \dot{\mathcal{Z}} = \{\mathcal{Z}, \mathcal{H}_p\}. \tag{28}$$

For (28) it is known that each subsystem can be solved exactly, so that Poisson-structure-preserving temporal semi-discrete methods can be constructed by composing the solutions of subsystems [23]. Moreover, we have the following proposition.

**Proposition 4.1** *For the Hamiltonian splitting (28) applied to the quasi-relativistic LP system, the charge $\int_{\Omega\times\mathbb{R}} f(x,p,t)\mathrm{d}x\mathrm{d}p$ and Poisson equation (5) (if satisfied initially) are conserved by the semi-discretization based on Hamiltonian splitting.*

Proof. *It is easy to know that the charge and Poisson equation are the two Casimir functionals corresponding to the Poisson bracket. By propositions 2.3 and 2.4 with $\Phi$ being an identity map, the two conservative quantities can be conserved by the Hamiltonian splitting methods.* □

**The subsystem corresponding to $\mathcal{H}_E$** is

$$\frac{\partial f}{\partial t} + E_x \frac{\partial f}{\partial p} = 0, \quad \frac{\partial E_x}{\partial t} = 0, \quad \frac{\partial \mathbf{E}_\perp}{\partial t} = 0, \quad \frac{\partial \mathbf{A}_\perp}{\partial t} = -\mathbf{E}_\perp. \tag{29}$$

For a given initial value $(f_0(x,p), E_{x0}(x), \mathbf{E}_{\perp 0}(x), \mathbf{A}_{\perp 0}(x))$ at time $t=0$, the solution of this subsystem at $t$ can be written as

$$\begin{aligned} &f(x,p,t) = f_0(x, p - tE_{x0}(x)), \quad E_x(x,t) = E_{x0}(x), \\ &\mathbf{E}_\perp(x,t) = \mathbf{E}_{\perp 0}(x), \quad \mathbf{A}_\perp(x,t) = \mathbf{A}_{\perp 0}(x) - t\mathbf{E}_{\perp 0}(x). \end{aligned} \tag{30}$$

From (30), it can be seen that $E_x$ and $\mathbf{E}_\perp$ stay unchanged along time, and the distribution $f$ is advected with constant velocity. In numerical computation, the distribution function $f$ can be advanced in time by reconstruction using the PSM method. Applying the Fourier expansion to the fourth equality of (30) gives the equality satisfied by the Fourier coefficients

$$\hat{\mathbf{A}}_{\perp,k}(t) = \hat{\mathbf{A}}_{\perp,k}(0) - t\hat{\mathbf{E}}_{\perp,k}(0).$$

It is clear from (30) that $\hat{E}_{x,k}(t) = \hat{E}_{x,k}(0)$. For this subsystem, we know that $\sum_{\ell=1}^N \hat{f}_{k,\ell}(t) = \sum_{\ell=1}^N \hat{f}_{k,\ell}(0)$, as PSM is charge-conserving. Assume initially the discrete Poisson equation is satisfied, i.e.

$$\frac{2\pi k\mathrm{i}}{L}\hat{E}_{x,k}(0) = \sum_{\ell=1}^N \hat{f}_{k,\ell}(0)\Delta p, k \neq 0, \text{and } \hat{E}_{x,0}(0) = 0. \tag{31}$$

then the discrete Poisson equation is satisfied at time $t$

$$\frac{2\pi k\mathrm{i}}{L}\hat{E}_{x,k}(t) = \sum_{\ell=1}^N \hat{f}_{k,\ell}(t)\Delta p,\ k \neq 0, \text{and } \hat{E}_{x,0}(t) = 0. \tag{32}$$

**The subsystem corresponding to $\mathcal{H}_A$** is

$$\frac{\partial f}{\partial t} - \mathbf{A}_\perp \cdot \frac{\partial \mathbf{A}_\perp}{\partial x}\frac{\partial f}{\partial p} = 0, \quad \frac{\partial E_x}{\partial t} = 0, \tag{33}$$

$$\frac{\partial \mathbf{E}_\perp}{\partial t} = -\frac{\partial^2 \mathbf{A}_\perp}{\partial x^2} + \mathbf{A}_\perp \int_{\mathbb{R}} f(x,p,t)\mathrm{d}p, \quad \frac{\partial \mathbf{A}_\perp}{\partial t} = 0. \tag{34}$$

With the initial value $(f_0(x,p),\ E_{x0}(x),\ \mathbf{E}_{\perp 0}(x),\ \mathbf{A}_{\perp 0}(x))$ at time $t=0$ the solution at time $t$ can be derived explicitly as

$$f(x,p,t) = f_0\left(x, p + t\mathbf{A}_{\perp 0}(x) \cdot \frac{\partial \mathbf{A}_{\perp 0}(x)}{\partial x}\right), \quad E_x(x,t) = E_{x0}(x),$$

$$\mathbf{E}_\perp(x,t) = \mathbf{E}_{\perp 0}(x) - t\frac{\partial^2 \mathbf{A}_{\perp 0}(x)}{\partial x^2} + t\mathbf{A}_{\perp 0}(x)\int_{\mathbb{R}} f_0(x,p)\mathrm{d}p, \quad \mathbf{A}_\perp(x,t) = \mathbf{A}_{\perp 0}(x).$$

The distribution function is advected with constant velocity $t\mathbf{A}_\perp(x_j,0)\cdot\frac{\partial\mathbf{A}_\perp}{\partial x}(x_j,0)$ in $p$ direction, which can be advanced in time by using PSM. By Fourier expansion, the Fourier coefficients of $\mathbf{E}_\perp$ are advanced as

$$\hat{\mathbf{E}}_{\perp,k}(t)=\hat{\mathbf{E}}_{\perp,k}(0)-t\left(\frac{2\pi\mathrm{i}k}{L}\right)^2\hat{\mathbf{A}}_{\perp,k}(0)+t\sum_{\ell=1}^{N}\sum_{\substack{k_1,k_2\in\mathbb{Z},k_1+k_2=k,\\ -M/2+1\le k_1,k_2\le M/2}}\Delta p\hat{\mathbf{A}}_{\perp,k_1}(0)\hat{f}_{k_2,\ell}(0).$$

Similar to the proof of subsystem $\mathcal{H}_E$, the discrete Poisson equation (32) is satisfied by the solution at $t$ of this subsystem if it is satisfied initially.

**The subsystem corresponding to $\mathcal{H}_p$** is

$$\frac{\partial f}{\partial t}+\frac{p}{\gamma_1}\frac{\partial f}{\partial x}=0,\quad \frac{\partial E_x}{\partial t}=-\int_{\mathbb{R}}\frac{p}{\gamma_1}f(x,p,t)\mathrm{d}p+\bar{J}(t),\quad \frac{\partial\mathbf{E}_\perp}{\partial t}=0,\quad \frac{\partial\mathbf{A}_\perp}{\partial t}=0. \tag{35}$$

With initial values $(f_0(x,p),E_{x0}(x),\mathbf{E}_{\perp0}(x),\mathbf{A}_{\perp0}(x))$ at time $t=0$, the solution is as follows,

$$f(x,p,t)=f_0\left(x-t\frac{p}{\gamma_1},p\right),\quad \mathbf{E}_\perp(x,t)=\mathbf{E}_{\perp0}(x),\quad \mathbf{A}_\perp(x,t)=\mathbf{A}_{\perp0}(x), \tag{36}$$

$$E_x(x,t)=E_{x0}(x)-\int_0^t\int_{\mathbb{R}}\frac{p}{\gamma_1}f(x,p,\tau)\mathrm{d}p\mathrm{d}\tau+\int_0^t\bar{J}(\tau)\mathrm{d}\tau. \tag{37}$$

To compute the distribution function, we apply the spectral expansion to the first equation of (36). Notice $\gamma_1=\sqrt{1+p^2}$, then

$$\hat{f}_{k,\ell}(t)=\hat{f}_{k,\ell}(0)\exp\left(-\mathrm{i}\frac{2\pi k}{L}t\frac{p_\ell}{\sqrt{1+p_\ell^2}}\right), \tag{38}$$

where $k=-M/2+1,\cdots,M/2,\ell=1,\ldots,N$. For $E_x$, when $k=0$ we have

$$\hat{E}_{x,0}(t)=\frac{1}{L}\int_\Omega E_x(x,t)\mathrm{d}x=0. \tag{39}$$

When $k\neq0$, using equation of (37) gives

$$\hat{E}_{x,k}(t)=\hat{E}_{x,k}(0)-\Delta p\int_0^t\sum_{\ell=1}^{N}\hat{f}_{k,\ell}(\tau)\frac{p_\ell}{\sqrt{1+p_\ell^2}}\mathrm{d}\tau.$$

Substituting (38) into the above equality, provides

$$\begin{aligned}\hat{E}_{x,k}(t) &= \hat{E}_{x,k}(0) - \Delta p \int_0^t \sum_{\ell=1}^{N} \hat{f}_{k,\ell}(0) \exp\left(-\mathrm{i}\frac{2\pi k}{L}\tau \frac{p_\ell}{\sqrt{1+p_\ell^2}}\right) \frac{p_\ell}{\sqrt{1+p_\ell^2}} \mathrm{d}\tau \\ &= \hat{E}_{x,k}(0) + \Delta p \frac{L}{2\pi \mathrm{i} k} \sum_{\ell=1}^{N} \hat{f}_{k,\ell}(0) \left[\exp\left(-\mathrm{i}\frac{2\pi k}{L} t \frac{p_\ell}{\sqrt{1+p_\ell^2}}\right) - 1\right].\end{aligned} \tag{40}$$

If initially the discrete Poisson equation $\frac{2\pi \mathrm{i} k}{L}\hat{E}_{x,k}(0) = \Delta p \sum_{\ell=1}^{N} \hat{f}_{k,\ell}(0)$ holds for $k \neq 0$. Then, inserting the relation into (40) gives

$$\begin{aligned}\hat{E}_{x,k}(t) &= \Delta p \frac{L}{2\pi \mathrm{i} k} \sum_{\ell=1}^{N} \hat{f}_{k,\ell}(0) \left[\exp\left(-\mathrm{i}\frac{2\pi}{L} k t \frac{p_\ell}{\sqrt{1+p_\ell^2}}\right)\right] \\ &= \Delta p \frac{L}{2\pi \mathrm{i} k} \sum_{\ell=1}^{N} \hat{f}_{k,\ell}(t).\end{aligned}$$

which is the discrete version of Poisson equation (32) at time $t$.

Based on the above Hamiltonian splitting methods in time, Fourier spectral method and finite volume methods in space, fully discrete schemes can be obtained by using composition methods [23].

**Proposition 4.2** *For the quasi-relativistic LP system, the solution of the above derived fully discrete scheme preserves the discrete charge*

$$\sum_{j=1}^{M}\sum_{\ell=1}^{N} f_{j,\ell}^{n+1} \Delta x \Delta p = \sum_{j=1}^{M}\sum_{\ell=1}^{N} f_{j,\ell}^{n} \Delta x \Delta p.$$

Proof. Due to the charge-conserving property of PSM, it can be seen from the construction of numerical methods that the discrete charge is conserved by the fully discrete solution of subsystems $\mathcal{H}_E$ and $\mathcal{H}_A$. As for subsystem $\mathcal{H}_p$, by the definition of fast Fourier transform, we have $\hat{f}_{0,\ell} = \sum_{j=1}^{M} f_{j,\ell}$. In order to prove the discrete charge conservation, we only need to prove that $\sum_{\ell=1}^{N} \hat{f}_{0,\ell}(t) = \sum_{\ell=1}^{N} \hat{f}_{0,\ell}(0)$, which is true from Eq. (38) when $k = 0$. □

**Proposition 4.3** *For the quasi-relativistic LP system, it can be proved that the fully discrete schemes constructed above preserves the discrete Poisson equation*

$$\begin{aligned} \frac{2\pi k\mathrm{i}}{L}\hat{E}^n_{x,k} &= \sum_{\ell=1}^{N} \hat{f}^n_{k,\ell}\Delta p, \ \textit{when } k \neq 0, \\ \hat{E}^n_{x,k} &= 0, \ \textit{when } k = 0. \end{aligned} \tag{41}$$

Proof. This can be proved by analyzing the fully discrete solution of each subsystem. □

*4.2. Fully relativistic case*

For the fully relativistic case, some subsystems obtained by Hamiltonian splitting methods are no longer solvable. Thus constructing numerical solutions to preserve the good conservative properties inherited by the original system becomes more important. In this subsection, we study the fully relativistic system by a conservative splitting [13, 24], which gives three one-dimensional conservative subsystems for Vlasov equation. By solving a succession of one dimensional problems, the approximate solution of distribution can be derived which is more efficient and easier to be implemented. The other advantages of the conservative splitting is that the discrete charge and the discrete Poisson equation are conserved.

Let $F = (\frac{p}{\gamma}, E_x - \frac{\mathbf{A}_\perp}{\gamma}\cdot\frac{\partial \mathbf{A}_\perp}{\partial x})^T$ be the $2D$ advective field of Vlasov equation Eq. (1). It is easy to check that $\nabla \cdot F = 0$ with $\nabla = (\frac{\partial}{\partial x}, \frac{\partial}{\partial p})^T$. So the Vlasov equation can be written in a conservative form

$$\frac{\partial f}{\partial t} + \frac{\partial}{\partial x}\left[\frac{p}{\gamma_1}f\right] + \frac{\partial}{\partial p}\left[\left(E_x - \frac{\mathbf{A}_\perp}{\gamma_2}\cdot\frac{\partial \mathbf{A}_\perp}{\partial x}\right)f\right] = 0.$$

Then, one conservative splitting for the evolutionary field of LP system (1-4)

is given by

$$\begin{pmatrix} -\frac{\partial}{\partial x}\left[\frac{p}{\gamma_1}f\right] - \frac{\partial}{\partial p}\left[\left(E_x - \frac{\mathbf{A}_\perp}{\gamma_2}\cdot\frac{\partial \mathbf{A}_\perp}{\partial x}\right)f\right] \\ -\frac{\partial^2 \mathbf{A}_\perp}{\partial x^2} + \mathbf{A}_\perp \int_{\mathbb{R}} \frac{1}{\gamma_2} f(x,p,t)\mathrm{d}p \\ -\mathbf{E}_\perp \\ -\int_{\mathbb{R}} \frac{p}{\gamma_1} f(x,p,t)\mathrm{d}p + \bar{J}(t) \end{pmatrix} = \underbrace{\begin{pmatrix} -\frac{\partial}{\partial p}\left(E_x f\right) \\ \mathbf{0} \\ -\mathbf{E}_\perp \\ 0 \end{pmatrix}}_{\mathcal{R}_E}$$
$$+ \underbrace{\begin{pmatrix} \frac{\partial}{\partial p}\left(\frac{1}{\gamma_2}\mathbf{A}_\perp \cdot \frac{\partial \mathbf{A}_\perp}{\partial x} f\right) \\ -\frac{\partial^2 \mathbf{A}_\perp}{\partial x^2} + \mathbf{A}_\perp \int_{\mathbb{R}} \frac{1}{\gamma_2} f(x,p,t)\mathrm{d}p \\ \mathbf{0} \\ 0 \end{pmatrix}}_{\mathcal{R}_A} + \underbrace{\begin{pmatrix} -\frac{\partial}{\partial x}\left(\frac{p}{\gamma_1} f\right) \\ \mathbf{0} \\ \mathbf{0} \\ -\int_{\mathbb{R}} \frac{p}{\gamma_1} f(x,p,t)\mathrm{d}p + \bar{J}(t) \end{pmatrix}}_{\mathcal{R}_p}. \tag{42}$$

It is noticed that the subsystem corresponding to $\mathcal{R}_E$ is the same as the one in the quasi-relativistic case. Thus, we concentrate on other two subsystems in this subsection.

**Remark 4.1** *The charge $\int_{\Omega\times\mathbb{R}} f(x,p,t)\mathrm{d}p\mathrm{d}x$ and Poisson equation (5) can be conserved by the solution of each subsystem when using the above conservative splitting.*

**The subsystem corresponding to $\mathcal{R}_A$** is

$$\frac{\partial f}{\partial t} - \frac{\partial}{\partial p}\left(\frac{1}{\gamma_2}\mathbf{A}_\perp \cdot \frac{\partial \mathbf{A}_\perp}{\partial x} f\right) = 0, \quad \frac{\partial \mathbf{A}_\perp}{\partial t} = 0, \tag{43}$$

$$\frac{\partial \mathbf{E}_\perp}{\partial t} = -\frac{\partial^2 \mathbf{A}_\perp}{\partial x^2} + \mathbf{A}_\perp \int_{\mathbb{R}} \frac{1}{\gamma_2} f(x,p,t)\mathrm{d}p, \quad \frac{\partial E_x}{\partial t} = 0, \tag{44}$$

where $\gamma_2 = \sqrt{1+p^2+|\mathbf{A}_\perp|^2}$. The characteristic equation of the first equation is

$$\dot{x}(t) = 0, \quad \dot{p}(t) = -\frac{1}{\sqrt{1+p^2(t)+|\mathbf{A}_\perp|^2(x,0)}}\mathbf{A}_\perp(x,0)\cdot\frac{\partial \mathbf{A}_\perp(x,0)}{\partial x}. \tag{45}$$

To solve (43) numerically, the numerical unknown $f_{j,\ell}(t)$ is obtained from the value of $f_{j,\ell}(0)$ thanks to the volume conservation property,

$$f_{j,\ell}(t) = \frac{1}{\Delta p}\int_{p_{\ell-\frac{1}{2}}(0)}^{p_{\ell+\frac{1}{2}}(0)} f_j(p,0)\mathrm{d}p,$$

where $p_{\ell\pm1/2}(0)$ is numerical solution of (45) solved by the fourth order Runge–Kutta method or other numerical methods in [13], and $f_j(p,0)$ is reconstructed from the integral average values $f_{j,\ell}(0)$ by using PSM. We approximate $\mathbf{E}_\perp$ by applying a trapezoidal integration to the first equation of (44),

$$\mathbf{E}_{\perp,j}(t) = \mathbf{E}_{\perp,j}(0) - t\frac{\partial^2 \mathbf{A}_\perp}{\partial x^2}(x_j,0) + t\mathbf{A}_{\perp,j}(0)\Delta p \sum_{\ell=1}^{N} \frac{1}{\gamma_{j,\ell}} \left( \frac{f_{j,\ell}(t) + f_{j,\ell}(0)}{2} \right)$$

where $\gamma_{j,\ell} = \sqrt{1 + p_\ell^2 + |\mathbf{A}_{\perp,j}(0)|^2}$. Due to the conservative method, we know that $\sum_{\ell=1}^{N} \hat{f}_{k,\ell}(t) = \sum_{\ell=1}^{N} \hat{f}_{k,\ell}(0)$. Notice $\hat{E}_{x,k}(t) = \hat{E}_{x,k}(0)$, then the discrete Poisson equation (32) is satisfied at time $t$ if it is satisfied initially.

**The subsystem corresponding to $\mathcal{R}_p$** is:

$$\frac{\partial f}{\partial t} + \frac{\partial}{\partial x}\left(\frac{p}{\gamma_1} f\right) = 0, \quad \frac{\partial \mathbf{E}_\perp}{\partial t} = 0, \tag{46}$$

$$\frac{\partial E_x}{\partial t} = -\int_{\mathbb{R}} \frac{p}{\gamma_1} f(x,p,t)\mathrm{d}p + \bar{J}(t), \quad \frac{\partial \mathbf{A}_\perp}{\partial t} = 0. \tag{47}$$

Apply the Fourier spectral method in $x$ direction and finite volume method in $p$ direction, we obtain the following equation in Fourier space,

$$\frac{\partial \hat{f}_{k,\ell}(t)}{\partial t} + \frac{2\pi \mathrm{i} k}{L} \widehat{\left(\frac{p_\ell}{\gamma_1} f_\ell(t)\right)}_k = 0, \tag{48}$$

where $k = -\frac{M}{2}+1, \cdots, \frac{M}{2}$, $\ell = 1, \cdots, N$. The second term of the above equality can be calculated further as

$$\widehat{\left(\frac{p_\ell}{\gamma_1} f_\ell(t)\right)}_k = \sum_{\substack{k_1,k_2\in\mathbb{Z}, k_1+k_2=k,\\ -M/2+1\le k_1,k_2\le M/2}} \widehat{\left(\frac{p_\ell}{\sqrt{1+p_\ell^2+|\mathbf{A}_\perp|^2}}\right)}_{k_1} \hat{f}_{k_2,\ell}(t).$$

For each $\ell$, it is known that Eq. (48) is a $M$-dimensional linear ordinary system about $\hat{\mathbf{f}}_\ell$ with $\hat{\mathbf{f}}_\ell = (\hat{f}_{-\frac{M}{2}+1,\ell}, \cdots, \hat{f}_{\frac{M}{2},\ell})^{\mathrm{T}}$, which can be solved exactly.

When $k = 0$, it is clear that

$$\hat{E}_{x,0}(t) = \frac{1}{L}\int_\Omega E(x,t)\mathrm{d}x = 0, \tag{49}$$

If $k \neq 0$, we express the first equation of Eq. (47) in Fourier space, and integrate it w.r.t time. Then, by using Eq. (48) we have

$$\begin{aligned}\hat{E}_{x,k}(t) &= \hat{E}_{x,k}(0) - \int_0^t \sum_{\ell=1}^{N} \widehat{\left(\frac{p_\ell}{\gamma_1} f_\ell(\tau)\right)}_k \Delta p d\tau \\ &= \hat{E}_{x,k}(0) + \frac{L}{2\pi \mathrm{i} k} \int_0^t \sum_{\ell=1}^{N} \frac{\partial \hat{f}_{k,\ell}(\tau)}{\partial t} \Delta p d\tau \\ &= \frac{L}{2\pi \mathrm{i} k} \sum_{\ell=1}^{N} \hat{f}_{k,\ell}(t)\Delta p + \hat{E}_{x,k}(0) - \frac{L}{2\pi \mathrm{i} k} \sum_{\ell=1}^{N} \hat{f}_{k,\ell}(0)\Delta p.\end{aligned}$$

This implies that

$$\hat{E}_{x,k}(t) - \frac{L}{2\pi \mathrm{i} k} \sum_{\ell=1}^{N} \hat{f}_{k,\ell}(t)\Delta p = \hat{E}_{x,k}(0) - \frac{L}{2\pi \mathrm{i} k} \sum_{\ell=1}^{N} \hat{f}_{k,\ell}(0)\Delta p,$$

which states the preservation of discrete Poisson equation if it is satisfied initially.

Based on the above conservative splitting methods in time, Fourier spectral method and finite volume methods in space, fully discrete schemes can be obtained by using composition methods [23].

**Proposition 4.4** *For the fully relativistic LP system, the above derived fully discrete schemes preserve the discrete charge*

$$\sum_{j=1}^{M}\sum_{\ell=1}^{N} f_{j,\ell}^{n+1}\Delta x \Delta p = \sum_{j=1}^{M}\sum_{\ell=1}^{N} f_{j,\ell}^{n}\Delta x \Delta p.$$

Proof. As subsystem $\mathcal{R}_E$ is the same as subsystem $\mathcal{H}_E$, the discrete charge is conserved by the fully discrete solution of this subsystem. Discrete charge is also conserved by the fully discrete solution of subsystem $\mathcal{R}_A$ due to the implementation of conservative splitting. For subsystem $\mathcal{R}_p$, we needs to prove that $\sum_{\ell=1}^{N} \hat{f}_{0,\ell}(t) = \sum_{\ell=1}^{N} \hat{f}_{0,\ell}(0)$, which is true from Eq. (48) when $k = 0$. □

**Proposition 4.5** *For the fully relativistic LP system, it can be proved that the solutions of the fully discrete schemes constructed above satisfy the discrete Poisson equation, for* $n \geq 1$

$$\begin{aligned} , \quad \frac{2\pi k\mathrm{i}}{L}\hat{E}^n_{x,k} &= \sum_{\ell=1}^{N} \hat{f}^n_{k,\ell}\Delta p, \ \textit{when } k \neq 0, \\ \hat{E}^n_{x,k} &= 0, \ \textit{when } k = 0. \end{aligned} \tag{50}$$

Proof. As mentioned above, the discrete Poisson equation (32) is satisfied by the fully discrete solution of each subsystem $\mathcal{R}_A$, $\mathcal{R}_p$, and $\mathcal{R}_E$ (the same as $\mathcal{H}_E$), discrete Poisson equation (32) is satisfied by the fully discrete schemes. □

## 5. Numerical experiments

In this section, we conduct the numerical simulations for the LP system both in quasi-relativistic and fully relativistic cases by using the numerical methods presented above. Moreover, comparisons with standard methods from references are presented.

### *5.1. Quasi-relativistic case*

Our first numerical experiment is to simulate the parametric instability phenomena during wave interaction. This phenomena happens, for instance, when electromagnetic waves propagate through a plasma layer (see [3, 24]). As a consequences of energy and momentum conservation, the waves allow the frequency and wavenumber matching.

In this numerical test, we take the initial distribution function as a homogeneous Maxwellian with a small perturbation which is expressed as

$$f_0(x,p) = \frac{1}{\sqrt{2\pi T}} \exp\left(-\frac{p^2}{2T}\right)(1 + a\cos(kx)),$$

where $T = 3/511$ denotes the temperature, $a = 0.001$ is the perturbation amplitude, $k = 1/\sqrt{2}$ is the wave number. The initial longitudinal electric field is taken as

$$E_{x0}(x) = \frac{a}{k}\sin(kx),$$

and the transverse circularly polarized electromagnetic field is

$$E_{y0}(x) = E_0 \cos(kx), \quad E_{z0}(x) = E_0 \sin(kx),$$
$$A_{y0}(x) = -E_0 \sin(kx), \quad A_{z0}(x) = E_0 \cos(kx)$$

with a quiver momentum $E_0 = \sqrt{3}$.

Using the Lie (first order) and Strang (second order) splitting for Hamiltonian splitting gives

$$\mathcal{Z}_{(n+1)\Delta t} = \phi_{\mathcal{H}_p,\Delta t} \circ \phi_{\mathcal{H}_E,\Delta t} \circ \phi_{\mathcal{H}_A,\Delta t} \mathcal{Z}_{n\Delta t},$$
$$\mathcal{Z}_{(n+1)\Delta t} = \phi_{\mathcal{H}_p,\Delta t/2} \circ \phi_{\mathcal{H}_E,\Delta t/2} \circ \phi_{\mathcal{H}_A,\Delta t} \circ \phi_{\mathcal{H}_E,\Delta t/2} \circ \phi_{\mathcal{H}_p,\Delta t/2} \mathcal{Z}_{n\Delta t},$$

where $\phi_{\mathcal{H}_E,t}$, $\phi_{\mathcal{H}_A,t}$ and $\phi_{\mathcal{H}_p,t}$ are the solution mappings of the subsystems corresponding to $\mathcal{H}_E$, $\mathcal{H}_A$, and $\mathcal{H}_p$.

We take the results from [6] as a comparison, in which a semi-Lagrangian method of second order in time is considered combined with the two-dimensional interpolation by cubic splines. The numerical parameters are chosen as $\Delta t = 0.02$, $\Omega \times \Omega_p = [0, 2\pi/k] \times [-\pi/k, \pi/k]$, and $M = N = 128$. First, we compare in Figs. 1-3 the results from [6] with those obtained by the Lie Hamiltonian splitting. From Fig. 1, it is investigated that the contour plots of distribution function $f$ by the two methods are similar. It shows that as time goes on there appear two vortices, which then separate.

We also compute the relative error of the total energy (16) and charge. The error of Poisson equation is measured by

$$\left( \sum_{j=1}^{M} \left( \left( \frac{\partial E_1^n}{\partial x_1} \right)_j - \sum_{\ell} f_{j,\ell}^n \Delta p + 1 \right)^2 \right)^{1/2}.$$

These results are displayed in Figs. 2 and 3. It is observed that using the semi-Lagrangian method [6] leads to a significant drift of errors after the instability starts ($t \approx 22$). In comparison, the Lie Hamiltonian splitting method gives better results: the relative charge is preserved in the level of $10^{-11}$; the relative energy error oscillates in the level of $10^{-3}$ over long time which is typical for geometric numerical integrations; the error of Poisson equation is about $10^{-10}$ which verifies that the discrete Poisson equation is satisfied by our numerical schemes. In Figs. 4 and 5, the results obtained by the Strang Hamiltonian splitting are displayed. In Figs 4, it shows that the Strang Hamiltonian splitting method gives the similar contour plots for the

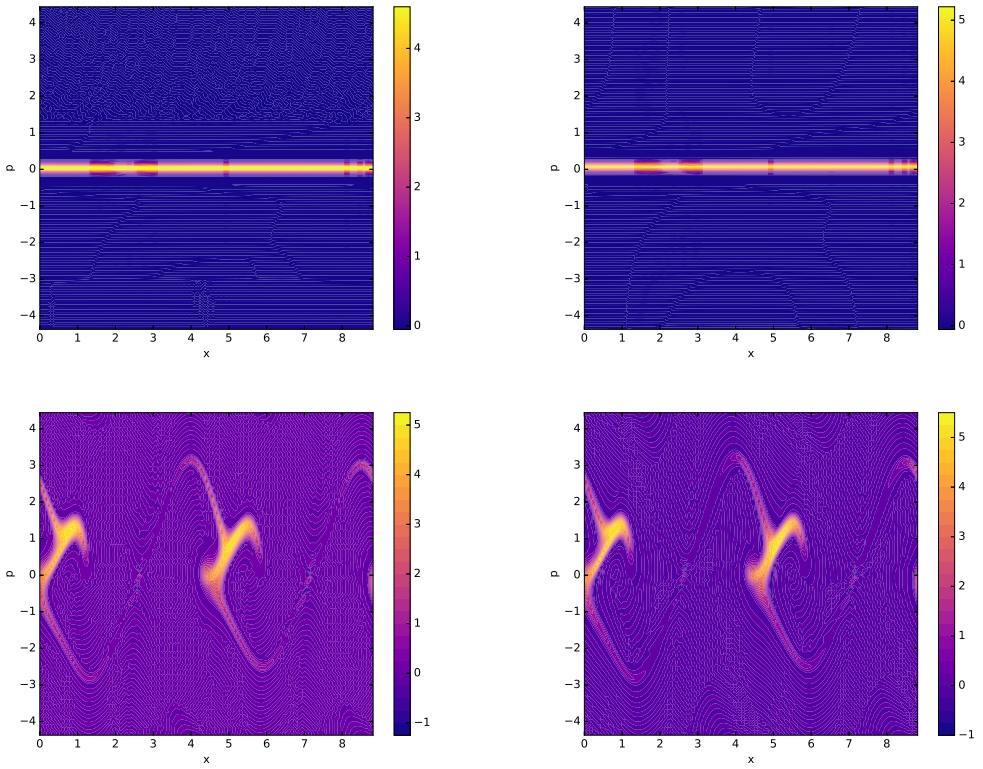


Figure 1: Quasi-relativistic case: time evolution of distribution function at $t = 10, 24$. Left: Lie Hamiltonian splitting method. Right: Semi-Lagrangian method.

distribution function as in Fig. 1. In Fig. 5, compared with the Lie Hamiltonian splitting, the error of total energy by Strang Hamiltonian splitting is smaller because of its second order of accuracy, which makes this method very attractive in numerical simulations.

*5.2. Fully relativistic case*

For the relativistic case, we simulate the vortices generated by an ultra-intense pump wave in a periodic box due to the relativistic parametric instability. In this numerical experiment, we use the same initial values as the ones in quasi-relativistic case except that the perturbation coefficient $a$ is taken as 0. The phase space domain is taken as $[0, 2\pi/k] \times [-\pi/k, \pi/k]$, the numbers of grids in phase space is $M = N = 128$, and $\Delta t$ is taken as 0.01. We split the fully relativistic LP system by conservative and advective

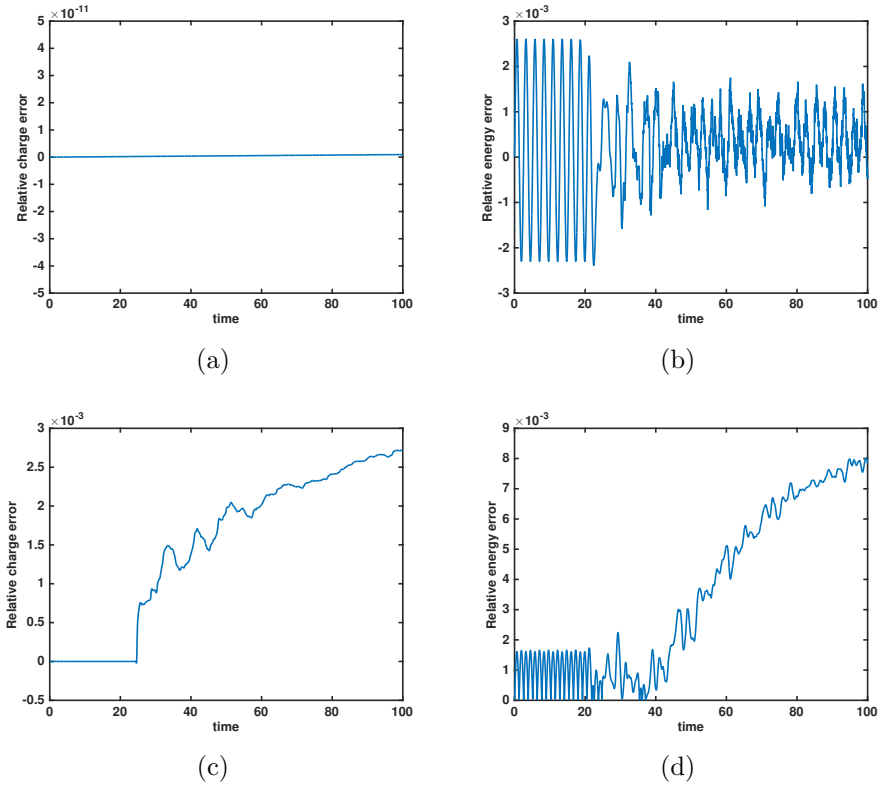


Figure 2: Quasi-relativistic case: time evolution of relative errors for charge, and energy computed by Lie Hamiltonian splitting method (a)-(b), and method in [6] (c)-(d).

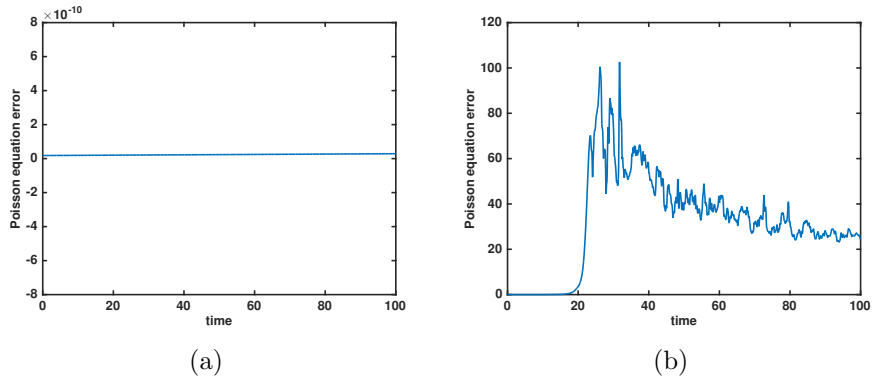


Figure 3: Quasi-relativistic case: time evolution of errors of Poisson equation by Lie Hamiltonian splitting method (a), and method in [6] (b).

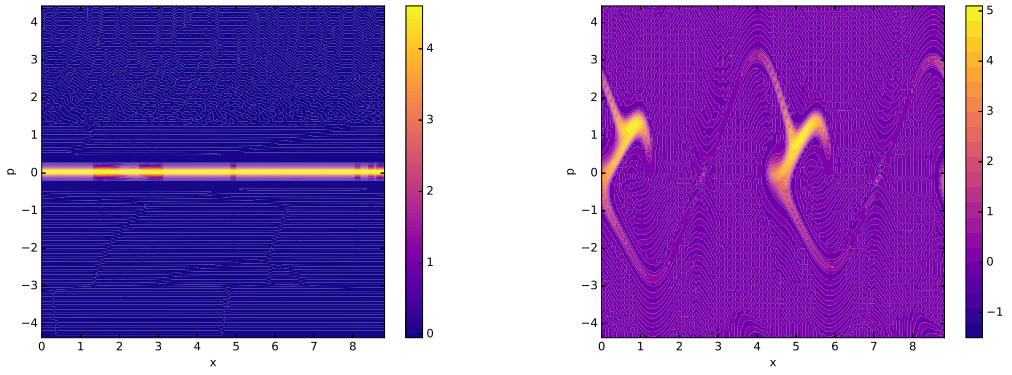


Figure 4: Quasi-relativistic case: time evolution of distribution function computed by Strang Hamiltonian splitting method at $t = 10$ and 24.

splittings, the resulting numerical discretizations in time are derived with Strang splitting method.

Similar behaviors of distribution function by the conservative and advective splittings are presented in Fig. 6. There appear two vertices firstly, then their structure becomes very complicated. This is in a very good agreement with the results obtained in [6]. We also compare the conservative splitting with the advective splitting by computing the relative errors for the charge, energy (given by (16)) and Poisson equation error, and the numerical results are shown in Figs. 7 and 8. From these figures, it can be seen that the conservative splitting gives better conservations of charge, energy and Poisson equation. Finally, the time evolutions for the second mode of $E_x$ and $E_y$ are displayed in Fig. 9 and 10. The dispersion analysis (see [19]) provides a growth rate of $\gamma = 0.409$ for the second mode of $E_x$ and a growth rate of $\gamma = 0.32$ for the second mode of $E_y$. Comparing Fig. 9 with Fig. 10, it is clear that the second modes of $E_x$ and $E_y$ by conservative splitting are in a better agreement with analytic results.

## 6. Conclusions

In this work, the Poisson structure of the LP system is investigated. Based on this structure, a Hamiltonian splitting method is given to numerically solve this system in the quasi-relativistic case. Fourier spectral and finite volume methods are used in phase space discretization. The scheme is applied

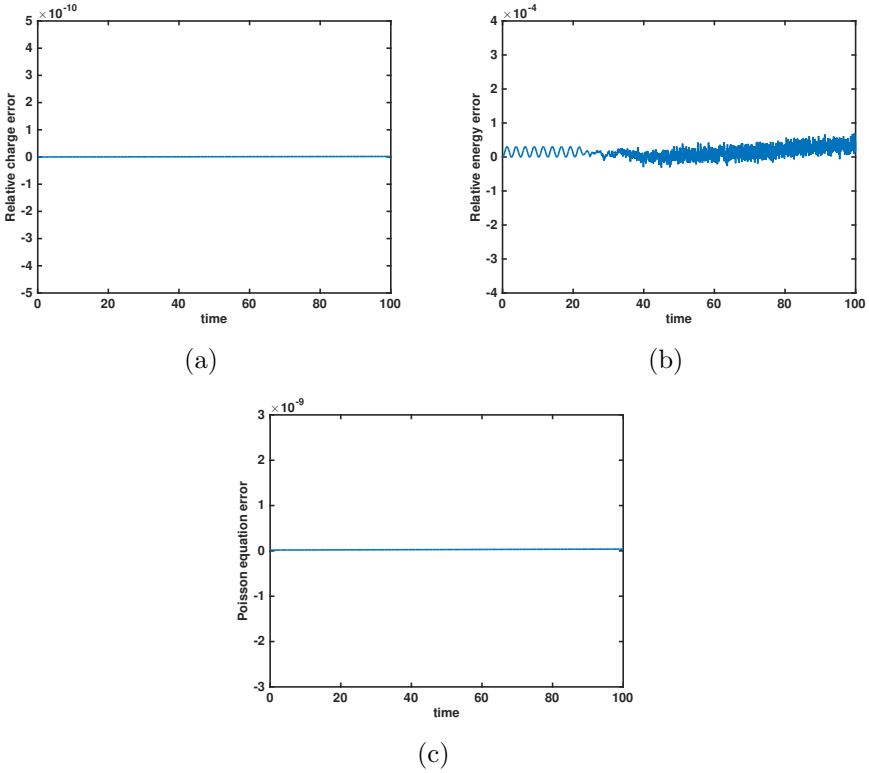


Figure 5: Quasi-relativistic case: time evolution of errors by Strang Hamiltonian splitting method. (a) Relative charge error; (b) Relative total energy error; (c) Poisson equation error.

in parametric instability, in which our scheme shows very good long term conservations of charge, energy and Poisson equation. The splitting method is extended into relativistic case by one conservative splitting.

There are several perspectives of this work that can be envisaged. First, application of this method to more complex laser-plasma numerical experiments can be conducted as in [3]. Second, more careful phase space discretizations can be considered to construct fully discrete energy preserving and Poisson-structure-preserving methods.

## Acknowledgements

We are grateful to anonymous referees for their useful comments. The first and second authors have been supported by the National Natural Science

Foundation of China 11771436, the ITER-China Program 2014GB124005. The third author was supported by the French ANR project Moonrise and has been supported by the French Federation for Magnetic Fusion Studies (FR-FCM) and by the Eurofusion consortium, and has received funding from the Euratom research and training programme 2014-2018 and 2019-2020 under grant agreement No. 633053. The views and opinions expressed herein do not necessarily reflect those of the European Commission.

## Appendix A. Proof of the Jacobi identity

The proof of Proposition 2.1.
As follows, we prove that the sum of terms 3, 7 and 9 vanishes.
For term 9, using the first and last equations in Eq. (14) leads to

$$\begin{aligned}
\text{Term } 9 + \text{cyc} &= \int_{\Omega\times\mathbb{R}} \frac{\delta\mathcal{H}}{\delta E_x}\frac{\partial f}{\partial p}\left(\frac{\delta\mathcal{F}}{\delta E_x}\frac{\partial}{\partial p}\frac{\delta\mathcal{G}}{\delta f} - \frac{\delta\mathcal{G}}{\delta E_x}\frac{\partial}{\partial p}\frac{\delta\mathcal{F}}{\delta f}\right)\mathrm{d}x\mathrm{d}p + \text{cyc} \\
&= \int_{\Omega\times\mathbb{R}} \Big(\underbrace{\frac{\delta\mathcal{F}}{\delta E_x}\frac{\partial}{\partial p}\frac{\delta\mathcal{G}}{\delta f}}_{9a} - \underbrace{\frac{\delta\mathcal{G}}{\delta E_x}\frac{\partial}{\partial p}\frac{\delta\mathcal{F}}{\delta f}}_{9b}\Big)\frac{\partial f}{\partial p}\frac{\delta\mathcal{H}}{\delta E_x}\mathrm{d}x\mathrm{d}p \\
&+ \int_{\Omega\times\mathbb{R}} \Big(\underbrace{\frac{\delta\mathcal{G}}{\delta E_x}\frac{\partial}{\partial p}\frac{\delta\mathcal{H}}{\delta f}}_{9c} - \underbrace{\frac{\delta\mathcal{H}}{\delta E_x}\frac{\partial}{\partial p}\frac{\delta\mathcal{G}}{\delta f}}_{9d}\Big)\frac{\partial f}{\partial p}\frac{\delta\mathcal{F}}{\delta E_x}\mathrm{d}x\mathrm{d}p \\
&+ \int_{\Omega\times\mathbb{R}} \Big(\underbrace{\frac{\delta\mathcal{H}}{\delta E_x}\frac{\partial}{\partial p}\frac{\delta\mathcal{F}}{\delta f}}_{9e} - \underbrace{\frac{\delta\mathcal{F}}{\delta E_x}\frac{\partial}{\partial p}\frac{\delta\mathcal{H}}{\delta f}}_{9f}\Big)\frac{\partial f}{\partial p}\frac{\delta\mathcal{G}}{\delta E_x}\mathrm{d}x\mathrm{d}p.
\end{aligned}$$

It vanishes as the terms 9a and 9d, 9b and 9e, 9c and 9f, are cancelled out.

Term 7 can be expanded as

$$
\begin{aligned}
\text{Term } 7 + \text{cyc} &= \int_{\Omega\times\mathbb{R}} f \left[\frac{\delta\{\mathcal{F},\mathcal{G}\}_{fE_x}}{\delta f}, \frac{\delta\mathcal{H}}{\delta f}\right]_{xp} \mathrm{d}x\mathrm{d}p + \text{cyc} \\
&= \int_{\Omega\times\mathbb{R}} f \frac{\partial}{\partial x}\left(\frac{\delta\mathcal{G}}{\delta E_x}\frac{\partial}{\partial p}\frac{\delta\mathcal{F}}{\delta f} - \frac{\delta\mathcal{G}}{\delta E_x}\frac{\partial}{\partial p}\frac{\delta\mathcal{F}}{\delta f}\right)\frac{\partial}{\partial p}\frac{\delta\mathcal{H}}{\delta f}\mathrm{d}x\mathrm{d}p \\
&- \int_{\Omega\times\mathbb{R}} f \frac{\partial}{\partial p}\left(\frac{\delta\mathcal{G}}{\delta E_x}\frac{\partial}{\partial p}\frac{\delta\mathcal{F}}{\delta f} - \frac{\delta\mathcal{F}}{\delta E_x}\frac{\partial}{\partial p}\frac{\delta\mathcal{G}}{\delta f}\right)\frac{\partial}{\partial x}\frac{\delta\mathcal{H}}{\delta f}\mathrm{d}x\mathrm{d}p + \text{cyc} \\
&= \int_{\Omega\times\mathbb{R}} \left(\frac{\delta\mathcal{G}}{\delta E_x}\frac{\partial}{\partial p}\frac{\delta\mathcal{F}}{\delta f} - \frac{\delta\mathcal{F}}{\delta E_x}\frac{\partial}{\partial p}\frac{\delta\mathcal{G}}{\delta f}\right)\left(\frac{\partial f}{\partial p}\frac{\partial}{\partial x}\frac{\delta\mathcal{H}}{\partial f} - \frac{\partial f}{\partial x}\frac{\partial}{\partial p}\frac{\delta\mathcal{H}}{\partial f}\right)\mathrm{d}x\mathrm{d}p + \text{cyc} \\
&= \int_{\Omega\times\mathbb{R}} \left(\frac{\delta\mathcal{G}}{\delta E_x}\frac{\partial}{\partial p}\frac{\delta\mathcal{F}}{\delta f} - \frac{\delta\mathcal{F}}{\delta E_x}\frac{\partial}{\partial p}\frac{\delta\mathcal{G}}{\delta f}\right)\Big(\frac{\partial f}{\partial p}\frac{\partial}{\partial x}\frac{\delta\mathcal{H}}{\partial f} - \underbrace{\frac{\partial f}{\partial x}\frac{\partial}{\partial p}\frac{\delta\mathcal{H}}{\partial f}}_{7a}\Big)\mathrm{d}x\mathrm{d}p \\
&+ \int_{\Omega\times\mathbb{R}} \left(\frac{\delta\mathcal{H}}{\delta E_x}\frac{\partial}{\partial p}\frac{\delta\mathcal{G}}{\delta f} - \frac{\delta\mathcal{G}}{\delta E_x}\frac{\partial}{\partial p}\frac{\delta\mathcal{H}}{\delta f}\right)\Big(\frac{\partial f}{\partial p}\frac{\partial}{\partial x}\frac{\delta\mathcal{F}}{\partial f} - \underbrace{\frac{\partial f}{\partial x}\frac{\partial}{\partial p}\frac{\delta\mathcal{F}}{\partial f}}_{7b}\Big)\mathrm{d}x\mathrm{d}p \\
&+ \int_{\Omega\times\mathbb{R}} \left(\frac{\delta\mathcal{F}}{\delta E_x}\frac{\partial}{\partial p}\frac{\delta\mathcal{H}}{\delta f} - \frac{\delta\mathcal{H}}{\delta E_x}\frac{\partial}{\partial p}\frac{\delta\mathcal{F}}{\delta f}\right)\Big(\frac{\partial f}{\partial p}\frac{\partial}{\partial x}\frac{\delta\mathcal{G}}{\partial f} - \underbrace{\frac{\partial f}{\partial x}\frac{\partial}{\partial p}\frac{\delta\mathcal{G}}{\partial f}}_{7c}\Big)\mathrm{d}x\mathrm{d}p.
\end{aligned}
\tag{A.1}
$$

Using the integrations by parts and the fact that the sum of Terms 7a, 7b, 7c is zero, provides

$$
\text{Term } 7 + \text{cyc} = \int_{\Omega\times\mathbb{R}} \left(\frac{\delta\mathcal{G}}{\delta E_x}\frac{\partial}{\partial p}\frac{\delta\mathcal{F}}{\delta f} - \frac{\delta\mathcal{F}}{\delta E_x}\frac{\partial}{\partial p}\frac{\delta\mathcal{G}}{\delta f}\right)\frac{\partial f}{\partial p}\frac{\partial}{\partial x}\frac{\delta\mathcal{H}}{\partial f}\mathrm{d}x\mathrm{d}p + \text{cyc}. \tag{A.2}
$$

Concerning Term 3, by using the first and fourth equations in Eq. (11) we have

$$
\text{Term } 3 + \text{cyc} = -\int_{\Omega\times\mathbb{R}} \frac{\delta\mathcal{H}}{\delta E_x}\frac{\partial f}{\partial p}\left[\frac{\delta\mathcal{F}}{\delta f}, \frac{\delta\mathcal{G}}{\delta f}\right]_{xp} \mathrm{d}x\mathrm{d}p + \text{cyc}. \tag{A.3}
$$

Taking the sum of Term 3 (A.3) and Term 7 (A.1) leads to

$$
\begin{aligned}
&\text{Term } 3 + \text{cyc} + \text{Term } 7 + \text{cyc} \\
&= \int_{\Omega\times\mathbb{R}} \left( \frac{\partial}{\partial p}\frac{\delta\mathcal{F}}{\delta f}\frac{\partial}{\partial x}\frac{\delta\mathcal{G}}{\delta f} - \frac{\partial}{\partial x}\frac{\delta\mathcal{F}}{\delta f}\frac{\partial}{\partial p}\frac{\delta\mathcal{G}}{\delta f} \right) \frac{\partial f}{\partial p}\frac{\delta\mathcal{H}}{\delta E_x}\mathrm{d}x\mathrm{d}p + \text{cyc} \\
&+ \int_{\Omega\times\mathbb{R}} \left( \frac{\delta\mathcal{G}}{\delta E_x}\frac{\partial}{\partial p}\frac{\delta\mathcal{F}}{\delta f} - \frac{\delta\mathcal{F}}{\delta E_x}\frac{\partial}{\partial p}\frac{\delta\mathcal{G}}{\delta f} \right) \frac{\partial f}{\partial p}\frac{\partial}{\partial x}\frac{\delta\mathcal{H}}{\delta f}\mathrm{d}x\mathrm{d}p + \text{cyc} \\
&= \int_{\Omega\times\mathbb{R}} \Big( \underbrace{\frac{\partial}{\partial p}\frac{\delta\mathcal{F}}{\delta f}\frac{\partial}{\partial x}\frac{\delta\mathcal{G}}{\delta f}}_{b} - \underbrace{\frac{\partial}{\partial x}\frac{\delta\mathcal{F}}{\delta f}\frac{\partial}{\partial p}\frac{\delta\mathcal{G}}{\delta f}}_{a} \Big) \frac{\partial f}{\partial p}\frac{\delta\mathcal{H}}{\delta E_x}\mathrm{d}x\mathrm{d}p \\
&+ \int_{\Omega\times\mathbb{R}} \Big( \underbrace{\frac{\partial}{\partial p}\frac{\delta\mathcal{G}}{\delta f}\frac{\partial}{\partial x}\frac{\delta\mathcal{H}}{\delta f}}_{d} - \underbrace{\frac{\partial}{\partial x}\frac{\delta\mathcal{G}}{\delta f}\frac{\partial}{\partial p}\frac{\delta\mathcal{H}}{\delta f}}_{c} \Big) \frac{\partial f}{\partial p}\frac{\delta\mathcal{F}}{\delta E_x}\mathrm{d}x\mathrm{d}p \\
&+ \int_{\Omega\times\mathbb{R}} \Big( \underbrace{\frac{\partial}{\partial p}\frac{\delta\mathcal{H}}{\delta f}\frac{\partial}{\partial x}\frac{\delta\mathcal{F}}{\delta f}}_{f} - \underbrace{\frac{\partial}{\partial x}\frac{\delta\mathcal{H}}{\delta f}\frac{\partial}{\partial p}\frac{\delta\mathcal{F}}{\delta f}}_{e} \Big) \frac{\partial f}{\partial p}\frac{\delta\mathcal{G}}{\delta E_x}\mathrm{d}x\mathrm{d}p \\
&+ \int_{\Omega\times\mathbb{R}} \Big( \underbrace{\frac{\delta\mathcal{G}}{\delta E_x}\frac{\partial}{\partial p}\frac{\delta\mathcal{F}}{\delta f}}_{e} - \underbrace{\frac{\delta\mathcal{F}}{\delta E_x}\frac{\partial}{\partial p}\frac{\delta\mathcal{G}}{\delta f}}_{d} \Big) \frac{\partial f}{\partial p}\frac{\partial}{\partial x}\frac{\delta\mathcal{H}}{\delta f}\mathrm{d}x\mathrm{d}p \\
&+ \int_{\Omega\times\mathbb{R}} \Big( \underbrace{\frac{\delta\mathcal{H}}{\delta E_x}\frac{\partial}{\partial p}\frac{\delta\mathcal{G}}{\delta f}}_{a} - \underbrace{\frac{\delta\mathcal{G}}{\delta E_x}\frac{\partial}{\partial p}\frac{\delta\mathcal{H}}{\delta f}}_{a} \Big) \frac{\partial f}{\partial p}\frac{\partial}{\partial x}\frac{\delta\mathcal{F}}{\delta f}\mathrm{d}x\mathrm{d}p \\
&+ \int_{\Omega\times\mathbb{R}} \Big( \underbrace{\frac{\delta\mathcal{F}}{\delta E_x}\frac{\partial}{\partial p}\frac{\delta\mathcal{H}}{\delta f}}_{c} - \underbrace{\frac{\delta\mathcal{H}}{\delta E_x}\frac{\partial}{\partial p}\frac{\delta\mathcal{F}}{\delta f}}_{b} \Big) \frac{\partial f}{\partial p}\frac{\partial}{\partial x}\frac{\delta\mathcal{G}}{\delta f}\mathrm{d}x\mathrm{d}p.
\end{aligned}
$$

The above terms vanish because of that the terms labelled by the same letter cancelled out.

## References


[1] J. Ackeret. Geometric integration of the Vlasov-Maxwell system with a variational particle-in-cell scheme. *Physics of Plasmas*, 19(8):83, 2012.

[2] M. L. Bégué, A. Ghizzo, P. Bertrand, E. Sonnendrücker, and O. Coulaud. Two-dimensional semi-lagrangian vlasov simulations of

laser–plasma interaction in the relativistic regime. *Journal of plasma physics*, 62(4):367–388, 1999.

[3] N. Besse, G. Latu, A. Ghizzo, E. Sonnendrucker, and P. Bertrand. A wavelet-MRA-based adaptive semi-Lagrangian method for the relativistic Vlasov-Maxwell system. *Journal of Computational Physics*, 227(16):7889–7916, 2008.

[4] C. K. Birdsall and A. B. Langdon. *Plasma Physics via Computer Simulation*. Institute of Physics Publishing, Philadelphia, PA, 1991.

[5] M. Bostan. Mild solutions for the relativistic Vlasov-Maxwell system for laser-plasma interaction. *Quarterly of Applied Mathematics*, 65(1):163–187, 2007.

[6] M. Bostan and N. Crouseilles. Convergence of a semi-Lagrangian scheme for the reduced VlasovMaxwell system for laserplasma interaction. *Numerische Mathematik*, 112(2):169–195, 2009.

[7] K. J. Bowers, B. J. Albright, L. Yin, B. Bergen, and T. J. T. Kwan. Ultrahigh performance three-dimensional electromagnetic relativistic kinetic plasma simulation. *Physics of Plasmas*, 15(5):055703, 2008.

[8] J. A. Carrillo and S. Labrunie. Global solutions for the one-dimensional Vlasov-Maxwell system for laser-plasma interaction. *Mathematical Models and Methods in Applied Sciences*, 16(1):19–57, 2006.

[9] C. Chandre and M. Perin. Hamiltonian reductions of the one-dimensional vlasov equation using phase-space moments. *Journal of Mathematical Physics*, 57(3):032902, 2016.

[10] Y. Cheng, A. Christlieb, and X. Zhong. Energy-conserving discontinuous Galerkin methods for the Vlasov-Ampère system. *Journal of Computational Physics*, 256:630–655, 2014.

[11] Y. Cheng, A. J. Christlieb, and X. Zhong. Energy-conserving discontinuous galerkin methods for the vlasov–maxwell system. *Journal of Computational Physics*, 279:145–173, 2014.

[12] N. Crouseilles, L. Einkemmer, and E. Faou. Hamiltonian splitting for the Vlasov-Maxwell equations. *Journal of Computational Physics*, 283:224–240, 2015.

[13] N. Crouseilles, M. Mehrenberger, and E. Sonnendrucker. Conservative semi-Lagrangian schemes for Vlasov equations. *Journal of Computational Physics*, 229(6):1927–1953, 2010.

[14] N. Crouseilles and T. Respaud. A charge preserving scheme for the numerical resolution of the Vlasov-Ampre equations. *Communications in Computational Physics*, 10(04):1001–1026, 2011.

[15] J. M. Dawson. Particle simulation of plasmas. *Reviews of Modern Physics*, 55(2):403–447, 1983.

[16] E. Evstatiev and B. Shadwick. Variational formulation of particle algorithms for kinetic plasma simulations. *Journal of Computational Physics*, 245(6):376–398, 2013.

[17] K. Feng and M. Qin. *Symplectic Geometric Algorithms for Hamiltonian Systems*. Springer Berlin Heidelberg, 2010.

[18] F. Filbet, E. Sonnendrucker, and P. Bertrand. Conservative numerical schemes for the Vlasov equation. *Journal of Computational Physics*, 172(1):166–187, 2001.

[19] A. Ghizzo, P. Bertrand, M. M. Shoucri, T. W. Johnston, E. Fualkow, and M. R. Feix. A Vlasov code for the numerical simulation of stimulated raman scattering. *Journal of Computational Physics*, 90(2):431–457, 1990.

[20] A. Ghizzo, D. Delsarto, T. Reveille, N. Besse, and R. Klein. Self-induced transparency scenario revisited via beat-wave heating induced by Doppler shift in overdense plasma layer. *Physics of Plasmas*, 14(6):062702, 2007.

[21] A. Ghizzo, F. Huot, and P. Bertrand. A non-periodic 2D semi-Lagrangian Vlasov code for laser–plasma interaction on parallel computer. *Journal of Computational Physics*, 186(1):47–69, 2003.

[22] A. Ghizzo, T. W. Johnston, T. Reveille, P. Bertrand, and M. Albrechtmarc. Stimulated-Raman-scatter behavior in a relativistically hot plasma slab and an electromagnetic low-order pseudocavity. *Physical Review E*, 74(4):046407, 2006.

[23] E. Hairer, C. Lubich, and G. Wanner. *Geometric Numerical Integration: structure-preserving algorithms for ordinary differential equations*, volume 31. Springer Science & Business Media, 2006.

[24] F. Huot, A. Ghizzo, P. Bertrand, E. Sonnendrucker, and O. Coulaud. Instability of the time splitting scheme for the one-dimensional and relativistic Vlasov-Maxwell system. *Journal of Computational Physics*, 185(2):512–531, 2003.

[25] M. Kraus, K. Kormann, P. J. Morrison, and E. Sonnendrücker. Gempic: Geometric electromagnetic particle-in-cell methods. *Journal of Plasma Physics*, 83(4), 2017.

[26] Y. Li, Y. He, Y. Sun, J. Niesen, H. Qin, and J. Liu. Solving the Vlasov–Maxwell equations using Hamiltonian splitting. *Journal of Computational Physics*, 396:381–399, 2019.

[27] J. E. Marsden and T. S. Ratiu. *Introduction to Mechanics and Symmetry*. Springer-Verlag, 1994.

[28] J. E. Marsden and A. Weinstein. The hamiltonian structure of the maxwell-vlasov equations. *Physica D: nonlinear phenomena*, 4(3):394–406, 1982.

[29] P. J. Morrison. A general theory for gauge-free lifting. *Physics of Plasmas*, 20(1):012104, 2013.

[30] P. J. Morrison. Structure and structure-preserving algorithms for plasma physics. *Physics of Plasmas*, 24(5):055502, 2017.

[31] H. Qin, J. Liu, J. Xiao, R. Zhang, Y. He, Y. Wang, Y. Sun, J. W. Burby, L. Ellison, and Y. Zhou. Canonical symplectic particle-in-cell method for long-term large-scale simulations of the Vlasov–Maxwell equations. *Nuclear Fusion*, 56(1):014001, 2015.

[32] R. D. Ruth. A Canonical Integration Technique. *IEEE Transactions on Nuclear Science*, 30(4):2669–2671, 1983.

[33] B. Shadwick, F. Lee, M. Tassi, and G. Tarkenton. Self-consistent hamiltonian model of beam transport in a laser-driven plasma accelerator. In *AIP Conference Proceedings*, volume 1299, pages 221–226. AIP, 2010.

[34] B. Shadwick, G. Tarkenton, E. Esarey, and F. M. Lee. Hamiltonian reductions for modeling relativistic laser-plasma interactions. *Communications in Nonlinear Science and Numerical Simulation*, 17(5):2153–2160, 2012.

[35] E. Sonnendrucker, J. Roche, P. Bertrand, and A. Ghizzo. The semi-Lagrangian method for the numerical resolution of the Vlasov equation. *Journal of Computational Physics*, 149(2):201–220, 1999.

[36] F. Vecil, P. M. Mestre, and S. Labrunie. WENO schemes applied to the quasi-relativistic Vlasov-Maxwell model for laserplasma interaction. *Comptes Rendus Mecanique*, 342(10):583–594, 2014.

[37] J. Xiao, J. Liu, H. Qin, and Z. Yu. A variational multi-symplectic particle-in-cell algorithm with smoothing functions for the Vlasov-Maxwell system. *Physics of Plasmas*, 20(10):2669–37, 2013.

[38] J. Xiao, H. Qin, J. Liu, Y. He, R. Zhang, and Y. Sun. Explicit high-order non-canonical symplectic particle-in-cell algorithms for Vlasov-Maxwell systems. *Physics of Plasmas*, 22(11):112504, 2015.

[39] M. Zerroukat, N. Wood, and A. Staniforth. The Parabolic Spline Method (PSM) for conservative transport problems. *International Journal for Numerical Methods in Fluids*, 51(11):1297–1318, 2006.

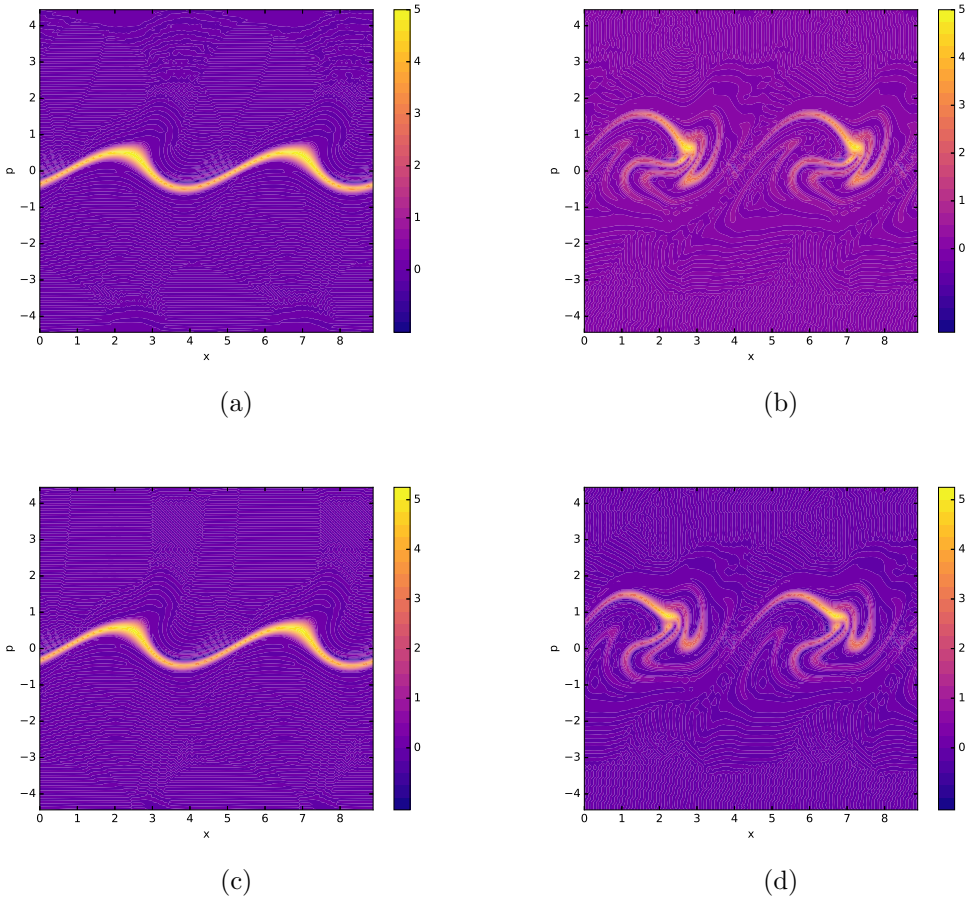


Figure 6: Fully relativistic case: time evolution of distribution function computed by Strang splitting for conservative splitting at $t = 136, 150$ (a)-(b) and advective splitting at $t = 125, 140$ (c)-(d).

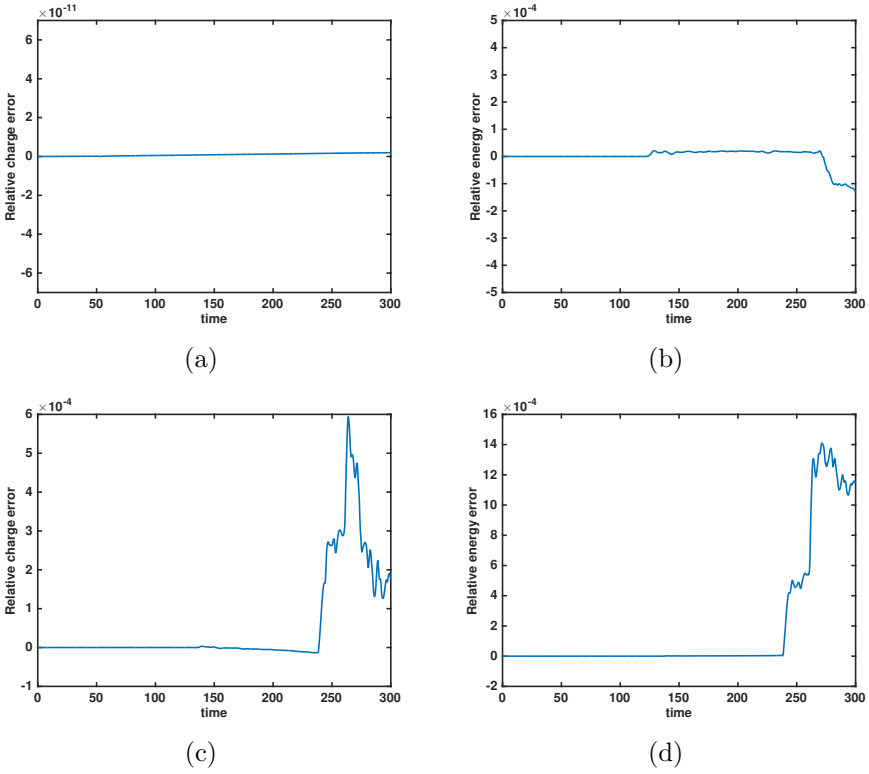


Figure 7: Fully relativistic case: time evolution of relative errors for charge, and total energy computed by Strang splitting for conservative splitting (a)-(b), and advective splitting (c)-(d).

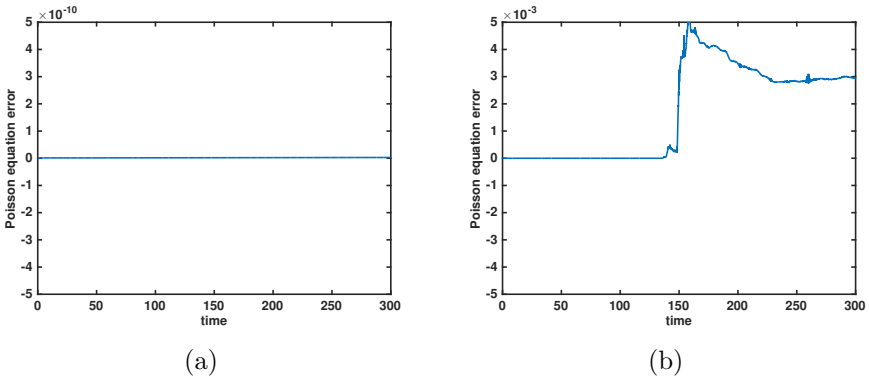


Figure 8: Fully relativistic case: time evolution of Poisson equation error computed by Strang splitting for conservative splitting (a) and advective splitting (b).

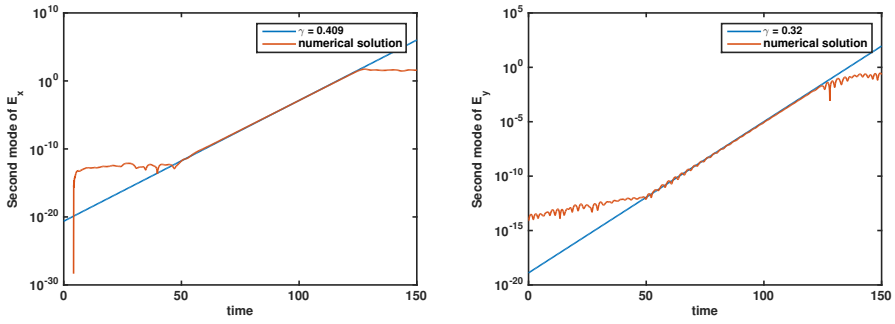


(a) (b)

Figure 9: Fully relativistic case: time evolution of second mode of (a) $E_x$ and (b) $E_y$ computed by Strang splitting for conservative splitting.

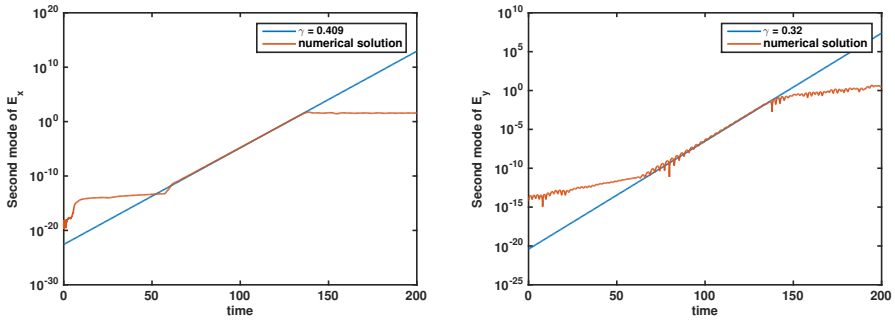


(a) (b)

Figure 10: Fully relativistic case: time evolution of second mode of (a) $E_x$ and (b) $E_y$ computed by Strang splitting for advective splitting.